# Integrated Arctic Observation System

Research and Innovation Action under EC Horizon2020
Grant Agreement no. 727890

Project coordinator:
Nansen Environmental and Remote Sensing Center, Norway

## Deliverable 3.13

## Final implementation and data: Distributed systems for ocean and sea ice

**Data delivery and report on results of the distributed systems for ocean and sea ice**

| | | | |
|---|---|---|---|
| Start date of project: | 01 December 2016 | Duration: | 60 months |
| Due date of deliverable: | May 31 2021 | Actual submission date: | 28 October 2021 |
| Lead beneficiary for preparing the deliverable: | | IOPAN | |
| Person-months used to produce deliverable: | | 46.3 pm | |

Authors: Agnieszka Beszczynska-Möller (IOPAN), Waldemar Walczowski (IOPAN), Bin Cheng (FMI), Roberta Pirazzini (FMI), Henna-Reetta Hannula (FMI), David Brus (FMI), Andrew King (NIVA), Kai Sørensen (NIVA), Bert van Bavel (NIVA), Sabine Marty (NIVA), Pierre Jaccard (NIVA), Marit Norli (NIVA), Elizaveta Protsenko (NIVA), Marie-Noelle Houssais (CNRS-LOCEAN), Christophe Herbaut (CNRS-LOCEAN), Laurent Mortier (CNRS-LOCEAN), Pierre Testor (CNRS-LOCEAN), Marcel Babin (CNRS-Takuvik), Claudie Marec (CNRS-Takuvik), Marie-Hélène Forget (CNRS-Takuvik), Achim Randelhoff (CNRS-Takuvik), with contribution from Hanne Sagen (NERSC) through the CAATEX project.

| Version | DATE | CHANGE RECORDS | LEAD AUTHOR |
|---|---|---|---|
| 1.0 | 01.03.2021 | Template | A. Beszczynska-Möller |
| | | Delivery date rescheduled to **30.09.2021** | Executive Board |
| 1.1 | 30.08.2021 | 1st draft | A. Beszczynska-Möller |
| 1.3 | 21.10.2021 | Final version | A. Beszczynska-Möller |
| 1.4 | 23.10.2021 | Revised version | S. Sandven |
| 1.5 | 28.10.2021 | Technical review and submission | K. Lygre |

| Approval | Date: | Sign. |
|---|---|---|
| X | 28. October 2021 | Stein Sandven<br>Coordinator |

| USED PERSON-MONTHS FOR THIS DELIVERABLE | | | | | |
|---|---|---|---|---|---|
| ***No*** | ***Beneficiary*** | ***PM*** | ***No*** | ***Beneficiary*** | ***PM*** |
| 1 | NERSC | *x* | 24 | TDUE | |
| 2 | UiB | | 25 | GINR | |
| 3 | IMR | | 48 | UNEXE | |
| 4 | MISU | | 27 | NIVA | *17* |
| 5 | AWI | | 28 | CNRS-LOCEAN | *7* |
| 6 | **IOPAN** | ***12*** | 29 | U Helsinki | |
| 7 | DTU | | 30 | GFZ | |
| 8 | AU | | 31 | ARMINES | |
| 9 | GEUS | | 32 | IGPAN | |
| 10 | FMI | *10.3* | 33 | U SLASKI | |
| 11 | UNIS | | 34 | BSC | |
| 12 | NORDECO | | 35 | DNV GL | |
| 13 | SMHI | | 36 | RIHMI-WDC | |
| 14 | USFD | | 37 | NIERSC | |
| 15 | NUIM | | 38 | WHOI | |
| 16 | IFREMER | | 39 | SIO | |
| 17 | MPG | | 40 | UAF | |
| 18 | EUROGOOS | | 41 | U Laval | |
| 19 | EUROCEAN | | 42 | ONC | |
| 20 | UPM | | 43 | NMEFC | |
| 21 | UB | | 44 | RADI | |
| 22 | UHAM | | 45 | KOPRI | |
| 23 | NORCE | | 46 | NIPR | |
| | | | 47 | PRIC | |

*x: contribution by the CAATEX project*

| DISSEMINATION LEVEL | | |
|---|---|---|
| PU | Public, fully open | **X** |
| CO | Confidential, restricted under conditions set out in Model Grant Agreement | |
| CI | Classified, information as referred to in Commission Decision 2001/844/EC | |

## *EXECUTIVE SUMMARY*

This document, ***Deliverable 3.13 - Final implementation of the observing system: Data delivery and report on results of the distributed observing systems for ocean and sea ice***, describes autonomous components of the Arctic observing system for ocean and sea ice measurements that were developed, tested, and implemented during the INTAROS field work seasons. Instruments and platforms described in D3.13 drifted freely on the sea ice or in the water column (ice tethered platforms, ice buoys and floats), moved along preprogrammed tracks (gliders) or measured autonomously at fixed locations (deep ocean moorings). An autonomous sensor package (FerryBox) and drone-based sensors were used to collect observations from the ships of opportunity or during large observing campaigns like MOSAiC. This document is intended to:

- Review status and performance of autonomous mobile and fixed observing platforms and sensors used for collecting ocean and sea ice observations in the Arctic during the INTAROS field work seasons.
- Describe performance and data obtained from the ice-tethered IAOOS-Equipex platform used for combined physical, atmospheric and sea ice measurements in the central Arctic Ocean.
- Describe performance and data collected with the deep ocean mooring deployed for the second INTAROS field season in the deep Nansen Basin.
- Describe performance and data collected by SIMBA (Snow and Ice Mass Balance Array) platforms for sea ice measurements, deployed with INTAROS contribution in the Arctic Ocean.
- Describe performance and data collected with new biogeochemical sensors for the FerryBox (pH/carbonate sensor, spectral absorption sensor and microplastic sampler) developed under INTAROS.
- Describe the performance of gliders and results from new endurance glider lines established under INTAROS in the northern Fram Strait.
- Describe INTAROS contribution to an array of BGC Argo floats in the Baffin Bay observatory, their performance, and collected data.
- Assess performance and fitness-to-purpose of the platforms, sensors and systems implemented under Task 3.4 for a future sustained Arctic observing system.

## Table of Contents

# 1. Introduction

The knowledge of physical and biological processes in the Arctic Ocean is limited because the ice cover severely hampers observations, both in the upper layers and deep waters. There is a severe lack of *in situ* multidisciplinary, in particular biogeochemical data for the Arctic Ocean and significant patterns of the Arctic ecosystem are not currently well monitored. Autonomous platforms for distributed observations (e.g. moorings, floats, ice-based observatories and gliders) can contribute year-round measurements over extended time periods from the most under-sampled regions of the Arctic Ocean.

The extensive overview of the current status of autonomous distributed platforms and systems for ocean and sea ice observations has been provided in the previous deliverables D.3.4 and D3.14. Selected components of this observing system were implemented during the INTAROS field seasons 2018-2019 and 2019-2020, in some cases preceded by earlier pilot experiments in the previous years. To extend the upper ocean, sea ice and atmospheric measurements in the central Arctic, one ice-tethered IAOOS-Equipex platform was deployed during the icebreaker Oden cruise ARCTIC2018. A deep ocean mooring equipped with BGC sensors was deployed for the second INTAROS field season in 2019 in the central Nansen Basin and recovered in 2020. INTAROS contributed to the array of over 38 SIMBA (Snow and Ice Mass Balance Array) buoys deployed in 2018-2020 during five campaigns on the central Arctic Ocean (NABOS 2018, CHINARE 2018, CAATEX 2019 and MOSAiC 2019 and 2020). Additional broadband and spectral surface albedo measurements were collected over the Arctic sea-ice during the MOSAiC campaign in 2020 with use of drones adapted for this purpose under INTAROS and additionally a broadband radiation station was deployed on ice in 2019-2020. New sensors and samplers that included a microplastics sampler, a combined pH/$CO_3$ sensor, and an integrated sphere absorption meter sensor have been developed and implemented for the FerryBox measurements along the endurance line between Tromsø and Ny Ålesund. Microplastic samples and pH measurements have been collected with the FerryBox during several repetitions of the Barents Sea Opening line since July 2018 and their analysis is ongoing while $CO_3$ part of the system and integrated sphere absorption meter sensor are partially operational and undergo final refinement before operational implementation. Glider measurements along the endurance lines were established and implemented for the summer and autumn missions in 2017-2020 along the Atlantic water pathways to the European Arctic in the northern Fram Strait. In addition to standard variables (temperature and salinity), the gliders also provided measurements of BGC variables as dissolved oxygen content, chl-a and CDOM fluorescence, and particulate backscattering. Geostrophic upper ocean currents were derived from the glider measurements and flight model. INTAROS contributed to an array of BGC Argo floats in Baffin Bay observatory where 17 floats deployed in 2016-2019 provided over 2000 profiles of key ocean physical (temperature and salinity) and biogeochemical (chl-a, CDOM, particle backscattering, dissolved oxygen, nitrate concentration, and radiation in 380 nm, 412 nm, 490 nm and PAR) variables. A large part of in situ observing activities described in this report will be continued beyond the INTAROS period under long-term initiatives and on-going and future projects. Deliverable 3.13 is concluded with assessment of the observing platforms, instruments, and samplers in terms of their applicability in a future sustained Arctic observing system and some technical recommendations are also provided.

# 2. Final implementation and operational use of the distributed observing systems for ocean and sea ice

The following work has been performed by partners responsible for Task 3.4.

## 2.1. IOPAN – ice-tethered IAOOS platform and deep ocean mooring in the Arctic Ocean

Contributors: Agnieszka Beszczynska-Möller, Waldemar Walczowski.

### 2.1.1. Results of the final implementation of the observing system

*Drifting ice-tethered IAOOS platform*

The INTAROS IAOOS-Equipex ice-tethered platform was deployed on 8 August 2018 during the Swedish icebreaker Oden cruise ARCTIC2018 in the central Arctic Ocean as a part of the North Pole drift ice station. The IAOOS-Equipex platform was deployed in the Amundsen basin close to the North Pole at the position 89.5553°N and 38.009°E by the IAOOS-Equipex technician from LOCEAN. The IAOOS-Equipex platform deployed under INTAROS was equipped with three separate sensor packages, dedicated to atmospheric, ocean and sea ice measurements. The instrument package consisted of microlidar and weather mast for atmospheric measurements, a CTDO profiler for ocean measurements, and a SIMBA-type instrument for sea ice measurements. The IAOOS platform drifted southward with Transpolar Drift and delivered the full data set for over 4 weeks after deployment, but transmission stopped afterwards, the most likely due to the damage by a polar bear. A detailed description of the IAOOS platform setup, instrumentation, drift trajectory, and measured data is provided in the INTAROS deliverable D3.14.

*Fixed deep ocean mooring deployed in the Nansen Basin*

After the failure of the IAOOS we decided to build a multipurpose oceanographic mooring for a yearlong deployment in the central part of the Arctic Ocean. The detailed justification for this change is described in the deliverable D3.14. The design of the mooring was done in collaboration with the CAATEX project. The INTAROS mooring is in many ways like the CAATEX moorings, but this mooring focus on combining physical, biogeochemical, and acoustic measurements.

Furthermore, the deep mooring (NERSC-4) complemented the INTAROS mooring line and the CAATEX moorings providing observations from a mooring array stretching from the INTAROS mooring array north of Svalbard deep into the Nansen Basin.

The INTAROS deep ocean mooring in the central Arctic Ocean was deployed in 2019 and recovered in 2020, supported by the CAATEX project using the Norwegian Coast Guard icebreaker *KV Svalbard*. The long oceanographic mooring (NERSC-4) was deployed in the deep Nansen Basin at the position 81° 47.094'N, 022° 00.280'E and water depth of 3458 m on 5 September 2019 during the CAATEX2019 cruise on *KV Svalbard* (see also section 2.6.1).

The INTAROS deep mooring labelled (according to the cruise naming scheme) NERSC-4 (Fig. 2.1.1) was equipped with the Nortek Signature 250 AD2CP for measuring the ocean currents in the upper layer and sea ice drift and draft (sea ice velocity and direction, and the depth of the ice keel as a proxy for ice thickness). Additionally, the deep mooring carried the TRDI LR-ADCP for ocean current profiling in the layer of a few hundred meters, nine instruments for ocean pressure, temperature, and salinity measurements (Seabird SBE37, RBR Concerto3 CTD and AADI SeaGuard), three instruments for dissolved oxygen and temperature measurements (RBBR Duo3 T.ODO and AADI SeaGuard, the latter also providing beam attenuation and point ocean current measurements), three clusters of double SAMI packages of pCO2 and pH sensors, 22 temperature sensors (RBR Solo3 or Duet3), AMAR passive acoustic recording system and NIOT acoustic passive receiving system with two hydrophones. The INTAROS deep mooring was a joint contribution from three INTAROS partners: IOPAN, NERSC and UiB-GFI with additional instrumentation from two external collaborators (FFI and NIOT).

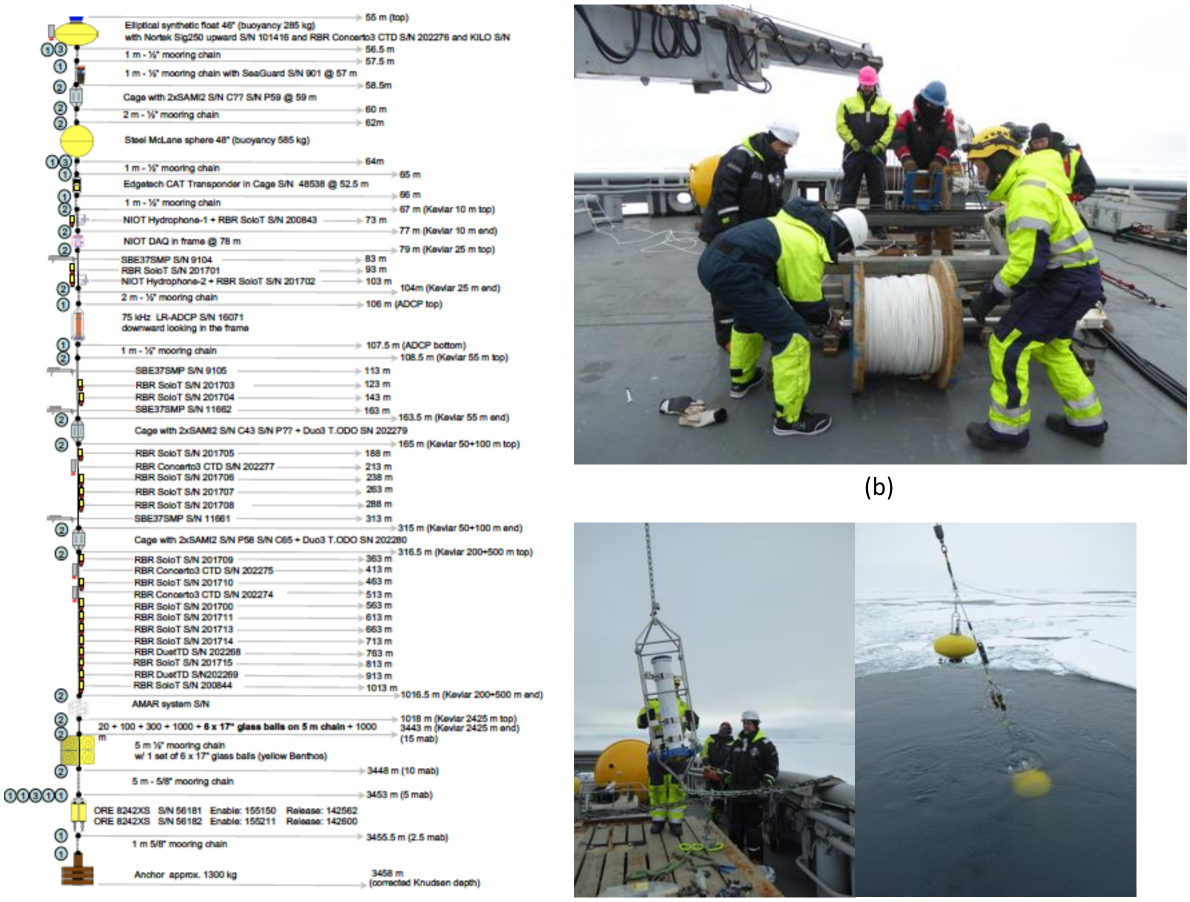


(b)

(a) (c)

***Figure 2.2.1.*** *(a) A schematic drawing of the INTAROS deep mooring NERSC-4 deployed in the Nansen Basin for the second INTAROS field season (2019-2020), (b) preparations and (c) mooring deployment operations from KV Svalbard in September 2019.*

The NERSC-4 deep mooring was recovered from under the ice during the CAATEX2020 cruise with KV Svalbard on 24 July 2020 (see also section 2.6.2). All instruments were retrieved in a good shape except one RBR temperature sensor that was lost during recovery. All instruments recorded the full time series of measured variables, covering the period from September 2019 to July 2020. Nortek Signature 250 was flooded when recovered but data has been recorded for the whole deployment period and were successfully retrieved from the instrument by manufacturer during the repair (albeit it resulted in much delayed data delivery).

The summary of data collected at the NERSC-4 mooring in the deep Nansen Basin, including measured variables and their details (depth, temporal and vertical resolution, and temporal coverage) is provided in Table 2.2.1.

*Table 2.1.1. Distribution of instruments for ocean physical measurements and details of measured variables at the IOPAN mooring NERSC-4 deployed in the deep Nansen Basin in 2019-2020.*

| Mooring | Mooring position and water depth | Instrument type | Measurement type<br>Nominal sensor depth<br>Profiling range<br>Bin size for profiles | Measured variables | Sampling period (s) | Start and stop of sampling (UTC) |
|---|---|---|---|---|---|---|
| **NERSC-4** | 81° 47.094'N<br>22° 00.280'E<br>3458 m | Nortek Signature 250 | Profile<br>34 m (depth)<br>4-32 m (range)<br>2 m bin size | Current velocity<br>Current direction<br>Sea ice drift and draft<br>Pressure (point)<br>Temperature (point) | 3600<br>3600<br>1<br>3600<br>3600 | 05.09.19 14:00<br>24.07.20 16:00 |
| | | RBR Concerto3 | Point measurement<br>36 m (depth) | Temperature<br>Salinity<br>Pressure | 600<br>600<br>600 | 05.09.19 14:00<br>24.07.20 16:00 |
| | | AADI SeaGuard | Point measurement<br>38 m (depth) | Temperature<br>Salinity<br>Pressure<br>Dissolved oxygen<br>Turbidity<br>Current velocity<br>Current direction | 3600<br>3600<br>3600<br>3600<br>3600<br>3600<br>3600 | 05.09.19 14:00<br>24.07.20 16:00 |
| | | RBR Solo3 | Point measurement<br>52 m (depth) | Temperature | 5 | 05.09.19 14:00<br>24.07.20 16:00 |
| | | SBE37 SMP | Point measurement<br>63 m | Temperature<br>Salinity<br>Pressure | 900<br>900<br>900 | 05.09.19 14:00<br>24.07.20 16:00 |
| | | RBR Solo3 | Point measurement<br>73 m (depth) | Temperature | 5 | 05.09.19 14:00<br>24.07.20 16:00 |
| | | RBR Solo3 | Point measurement<br>83 m (depth) | Temperature | 5 | 05.09.19 14:00<br>24.07.20 16:00 |
| | | TRDI LRADCP 75 kHz | Profile<br>34 m (depth)<br>100-400/500 m (range)<br>16 m bin size | Current velocity<br>Current direction<br>Pressure (point)<br>Temperature (point) | 3600<br>3600<br>3600<br>3600 | 05.09.19 14:00<br>24.07.20 16:00 |
| | | SBE37 SMP | Point measurement<br>93 m | Temperature<br>Salinity<br>Pressure | 900<br>900<br>900 | 05.09.19 14:00<br>24.07.20 16:00 |
| | | RBR Solo3 | Point measurement<br>103 m (depth) | Temperature | 5 | 05.09.19 14:00<br>24.07.20 16:00 |
| | | RBR Solo3 | Point measurement<br>123 m (depth) | Temperature | 5 | 05.09.19 14:00<br>24.07.20 16:00 |
| | | SBE37 SMP | Point measurement<br>143 m | Temperature<br>Salinity<br>Pressure | 900<br>900<br>900 | 05.09.19 14:00<br>24.07.20 16:00 |
| | | RBR Duo3 T.ODO | Point measurement<br>144 m | Temperature<br>Dissolved oxygen | 1200<br>1200 | 05.09.19 14:00<br>24.07.20 16:00 |
| | | RBR Solo3 | Point measurement<br>168 m (depth) | Temperature | 5 | 05.09.19 14:00<br>24.07.20 16:00 |
| | | RBR Concerto3 | Point measurement<br>193 m (depth) | Temperature<br>Salinity<br>Pressure | 600<br>600<br>600 | 05.09.19 14:00<br>24.07.20 16:00 |
| | | RBR Solo3 | Point measurement<br>218 m (depth) | Temperature | 5 | 05.09.19 14:00<br>24.07.20 16:00 |
| | | RBR Solo3 | Point measurement<br>243 m (depth) | Temperature | 5 | 05.09.19 14:00<br>24.07.20 16:00 |

| | | | | | | |
|---|---|---|---|---|---|---|
| | | RBR Solo3 | Point measurement<br>268 m (depth) | Temperature | 5 | 05.09.19 14:00<br>24.07.20 16:00 |
| | | SBE37 SMP | Point measurement<br>293 m (depth) | Temperature<br>Salinity<br>Pressure | 900<br>900<br>900 | 05.09.19 14:00<br>24.07.20 16:00 |
| | | RBR Duo3<br>T.ODO | Point measurement<br>296 m | Temperature<br>Dissolved oxygen | 1200<br>1200 | 05.09.19 14:00<br>24.07.20 16:00 |
| | | RBR Solo3 | Point measurement<br>343 m (depth) | Temperature | 5 | 05.09.19 14:00<br>24.07.20 16:00 |
| | | RBR<br>Concerto3 | Point measurement<br>393 m (depth) | Temperature<br>Salinity<br>Pressure | 600<br>600<br>600 | 05.09.19 14:00<br>24.07.20 16:00 |
| | | RBR Solo3 | Point measurement<br>443 m (depth) | Temperature | 5 | 05.09.19 14:00<br>24.07.20 16:00 |
| | | RBR<br>Concerto3 | Point measurement<br>493 m (depth) | Temperature<br>Salinity<br>Pressure | 600<br>600<br>600 | 05.09.19 14:00<br>24.07.20 16:00 |
| | | RBR Solo3 | Point measurement<br>543 m (depth) | Temperature | 5 | 05.09.19 14:00<br>24.07.20 16:00 |
| | | RBR Solo3 | Point measurement<br>593 m (depth) | Temperature | 5 | 05.09.19 14:00<br>24.07.20 16:00 |
| | | RBR Solo3 | Point measurement<br>643 m (depth) | Temperature | 5 | 05.09.19 14:00<br>24.07.20 16:00 |
| | | RBR Solo3 | Point measurement<br>693 m (depth) | Temperature | 5 | 05.09.19 14:00<br>24.07.20 16:00 |
| | | RBR Duet3 | Point measurement<br>743 m (depth) | Temperature<br>Pressure | 10<br>10 | 05.09.19 14:00<br>24.07.20 16:00 |
| | | RBR Solo3 | Point measurement<br>793 m (depth) | Temperature | 5 | 05.09.19 14:00<br>24.07.20 16:00 |
| | | RBR Duet3 | Point measurement<br>893 m (depth) | Temperature<br>Pressure | 10<br>10 | 05.09.19 14:00<br>24.07.20 16:00 |
| | | RBR Solo3 | Point measurement<br>993 m (depth) | Temperature | 5 | 05.09.19 14:00<br>24.07.20 16:00 |
| | | RBR Duet3 | Point measurement<br>1417 m (depth) | Temperature<br>Pressure | 10<br>10 | 05.09.19 14:00<br>24.07.20 16:00 |
| | | RBR Duet3 | Point measurement<br>2417 m (depth) | Temperature<br>Pressure | 10<br>10 | Lost during<br>recovery |
| | | RBR Solo3 | Point measurement<br>3422 m (depth) | Temperature | 5 | 05.09.19 14:00<br>24.07.20 16:00 |

### 2.1.2. Lessons learned and technology challenges identified during the project

*Drifting ice-tethered IAOOS platform*

The IAOOS ice-tethered platform was deployed for INTAROS by the experienced IAOOS team (the same group which developed and built the platform) in optimal sea ice conditions on the carefully selected ice floe. Despite of these efforts, the lifetime of the platform was unexpectedly short and a technical failure due to mechanical damage by a polar bear was the most likely cause. This sort of accidents cannot be unfortunately foreseen and has been for long time one of most common dangers to the equipment drifting for long time on sea ice in remote areas. Future efforts should include development of better protection of the on-ice components of the platform against polar bears and other physical damage (improving robustness of the outer shell, deterrent system against polar bears). A duplication of a communication (positioning and data transfer) system would be advantageous, taken that the power supply is independent for both systems (main and backup). More generally, the heavily instrumented multidisciplinary ice-tethered platforms provide a benefit of concurrent collection of different data types (ocean, atmospheric, sea ice, sometimes also biogeochemical data) but they are also increasingly expensive. Taking into account the potential high risk of ice-tethered deployments in the central Arctic, a future observing system should be perhaps composed of a higher number of simpler, more robust, lower cost ice-tethered platforms measuring a basic suite of ocean key physical variables with better coverage (and therefore limited data loss if a single platform is lost) and a smaller number of experimental, multiparameter platforms with a more sophisticated (and costly) backup systems for data retrieval. Development of a future ice-tethered platform that will be robust, affordable, and operable by different groups and can be more widely used in the Arctic Ocean requires a dedicated long-term effort and cannot be achieved within a single project.

*Deep ocean mooring deployed in the Nansen Basin*

The main lesson learned from deployment of the deep ocean mooring in the Nansen Basin was a critical need for collaboration among different partners, projects, and infrastructure operators with activities in the remote areas of the Arctic Ocean. The mooring operations for deployment and recovery of the deep INTAROS mooring were only possible thanks to excellent collaboration with the Norwegian-US project CAATEX (see Section 2.6) and the Norwegian Coast Guard providing ship time of their icebreaker KV Svalbard and full technical and personnel support for mooring operations.

Technology challenges for the deep mooring in the Nansen Basin are like those found for the INTAROS moorings north of Svalbard (described in more details in the deliverable D.3.11) and in general, all moorings in seasonally ice-covered regions of the Arctic Ocean. Additionally, a deep mooring (at the water depth over 3000 m) deployed in an ice-covered location requires a special attention in terms of moorings design and deployment/recovery procedures. For mooring operations, the navigational and ice management skills of the vessel officers are of the uttermost importance to optimally plan and use the limited open space in drifting ice. Under-ice positioning and locating aids (acoustic pingers, avalanche beacons) are crucial for the safe mooring recovery when stuck under the ice floes. Since floatation elements and cages carrying instruments usually surface between or under ice floes, good protection of vulnerable sensors is highly important. Our experience shows also that data should be read out and secured immediately after recovery because of possibility of instrument damage (and e.g., consequent leakage) during recovery in ice. General experience from deployments in the remote, difficult to access Arctic regions highlights the need of using double acoustic releases (if available), equipped with battery packs ensuring their lifetime at least 1-2 years longer than the planned deployment period. Similarly, instruments should be programmed with a safety margin of another year (field season) in the case if a planned mooring recovery is not feasible due to difficult ice condition and inaccessibility of mooring location (even if it is done at the cost of lower temporal resolution of measurements).

Sharing the mooring infrastructure by several partners, bringing in instruments measuring different ocean and sea ice variables, has a significant advantage of concurrent observations of different types (e.g., ocean physical and biogeochemical parameters, and acoustic passive recordings) which allow for more comprehensive analysis and interpretation of obtained observations. The deep INTAROS mooring was one of the very few examples of collaborative multidisciplinary continuous year-round measurements in the fixed location in the deep Arctic basin and as such provides a model for efficient co-using of infrastructure in a future Arctic observing system.

### 2.1.3. Description of processing and analysis of the obtained data

*Deep ocean mooring deployed in the Nansen Basin*

SBE37 raw time series of temperature, conductivity and pressure are processed according to the standard procedure that includes data conversion into engineering units, despiking, averaging onto 1 hour interval, and calculating derived variables (salinity and potential density). Processed data are archived as Matlab files and finally as netCDF files, including the full metadata set. Each netCDF file contains processed data from all SBE37 instruments located on a single mooring. Similar processing procedure is applied to RBR Concerto3 data sets.

Similar procedure is applied to RBR temperature sensors Solo3 or temperature and pressure sensors Duet3. Data processing steps include data conversion into engineering units, despiking, averaging onto 1 hour interval, and calculating derived variables (depth, only for Duet). Processed data are archived as Matlab files and finally as netCDF files, including the full metadata set. Each netCDF file contains processed data from all RBR Solo and Duet instruments located on a single mooring.

Processing of ADCP data from the IOPAN moorings starts with the steps specific to different types of ADCPs (Nortek Signature 250 and TRDI LR-ADCP), including extraction of data from the ADCP binary files and conversion to engineering units. Further steps are similar for all ADCPs and include correction for magnetic declination, quality control procedures and re-mapping on the constant depth levels. The workflow for ADCP data post-processing and quality control consists of following steps:

– Magnetic declination correction and direction test,
– In and out the water test,
– Calculating distance from the surface to the center of each depth cell,
– Tilting angle and side lobe test,
– Coarse outlier removal,
– Tests of additional parameters (echo intensity, correlation magnitude, percent of good, error velocity and vertical velocity) to identify potentially bad data,
– Re-mapping data on uniform depth levels,

– Archiving processed data as Matlab files and finally as netCDF files, including the full metadata set.

Processing of sea ice drift and draft (ice keel depth) data from Nortek Signature 250 is still under development, using the instrument capability of automatic ‘ice tracking’ using the acoustic surface tracking (AST) by finding the range of the acoustic echo indicating the water-ice interface (ice cover) by locating the leading edge of the peak of the return acoustic signal. In general, the measurement of ice thickness is made by subtracting the location of the leading edge of the AST peak from the mean depth determined from a pressure measurement (also made by Signature 250) after all corrections which include corrections for atmospheric pressure fluctuations, temperature and salinity, sound speed, and instrument tilt.

### 2.1.4. Accessibility of the obtained data sets and repositories used

*Drifting ice-tethered IAOOS platform*

The raw data set from the INTAROS IAOOS-Equipex platform is stored and available upon request on the IOPAN ftp server (IP: 153.19.130.250, user: iaoos-data, password protected). The data processing is ongoing and the final processed data sets (physical variables) will be registered in the INTAROS data catalogue and submitted to the IOPAN eCUDO open data base at the end of 2021.

*Deep ocean mooring deployed in the Nansen Basin*

Processed data from all instruments at the NERSC-4 mooring will be archived in the netCDF format with full metadata set. The structure and content of metadata in netCDF files and variable structure is currently under development by the dedicated INTAROS working group and will be soon established for all types of measurements collected by moored instrumentation. When data processing and conversion into netCDF files is finished, data from IOPAN moorings will be archived in the Oceanographic Data and Information System eCUDO (Polish national data base for oceanographic data) with an individual DOI number for each netCDF file. Data will be publicly available from eCUDO after publication of planned INTAROS papers in the INTAROS Ocean Sciences Special Issue.

### 2.1.5. Future plans for operation of the observing system, including data provision

*Drifting ice-tethered IAOOS platform*

Currently there are no plans for further deployments of ice-tethered platforms (IAOOS or ITPs) by Task 3.4 partners beyond the INTAROS period. This activity requires a dedicated long-term effort and extensive resources with sustained dedicated funding that are not currently available in the INTAROS consortium.

*Deep ocean mooring deployed in the Nansen Basin*

The INTAROS deep ocean moorings were operated during INTAROS due to the opportunity of deployment and recovery provided by the CAATEX project. While currently there are no plans for further deployments in the deep Nansen Basin, the deep mooring can be in future deployed on opportunistic basis, taking an advantage of other cruises and campaigns in the Eurasian Basin. INTAROS moorings will be continued north of Svalbard under collaboration with the Norwegian Nansen Legacy program and A-TWAIN project. There is a possibility that the A-TWAIN array will be extended northward and the INTAROS legacy mooring will be deployed in future as a deepest seaward A-TWAIN mooring.

*Data exploitation.* Data collected at the INTAROS deep mooring (also the shorter time series of data from ice-tethered platform) will be used in further research activities focused on the ocean physical state and dynamics in the deep Arctic basins. Time series of variables measured by moored instruments can be also used to provide derived products for other research activities, e.g. environmental background for biological or carbon system studies in the central Arctic. Potential users include scientists across a wide range of different disciplines, including modelers working with ocean and climate forecast and prediction or groups working on assessments of Arctic ecosystems and natural resources. Interactions between ocean and sea ice and ocean-ice statistics in poorly observed deep parts of the Arctic Ocean can be of a special interest for planning and operating future shipping routes in the opening for navigation Arctic areas.

## 2.2. FMI – SIMBA buoys in the Arctic Ocean and fixed station and UAV-based radiation measurements during MOSAiC

Contributors to SIMBA snow and ice mass balance buoys: Bin Cheng.

Contributors to Fixed station and UAV-based radiation measurements during the MOSAiC expedition: Roberta Pirazzini, Henna-Reetta Hannula, David Brus.

### 2.2.1. Results of the final implementation of the observing system - SIMBA snow and ice mass balance buoys

During INTAROS, several high-profile international Arctic field campaigns have been carried out. Up to 38 SIMBA buoys have been deployed in different regions in the Arctic Ocean and drifted along with the ice floes. The average working time of SIMBA buoy is about one year depending on the in-situ environment and configurations of data acquisition frequency. The SIMBA drift trajectories follow mainly the Beaufort Gyre and the Transpolar Drift Stream (Fig.2.2.1).

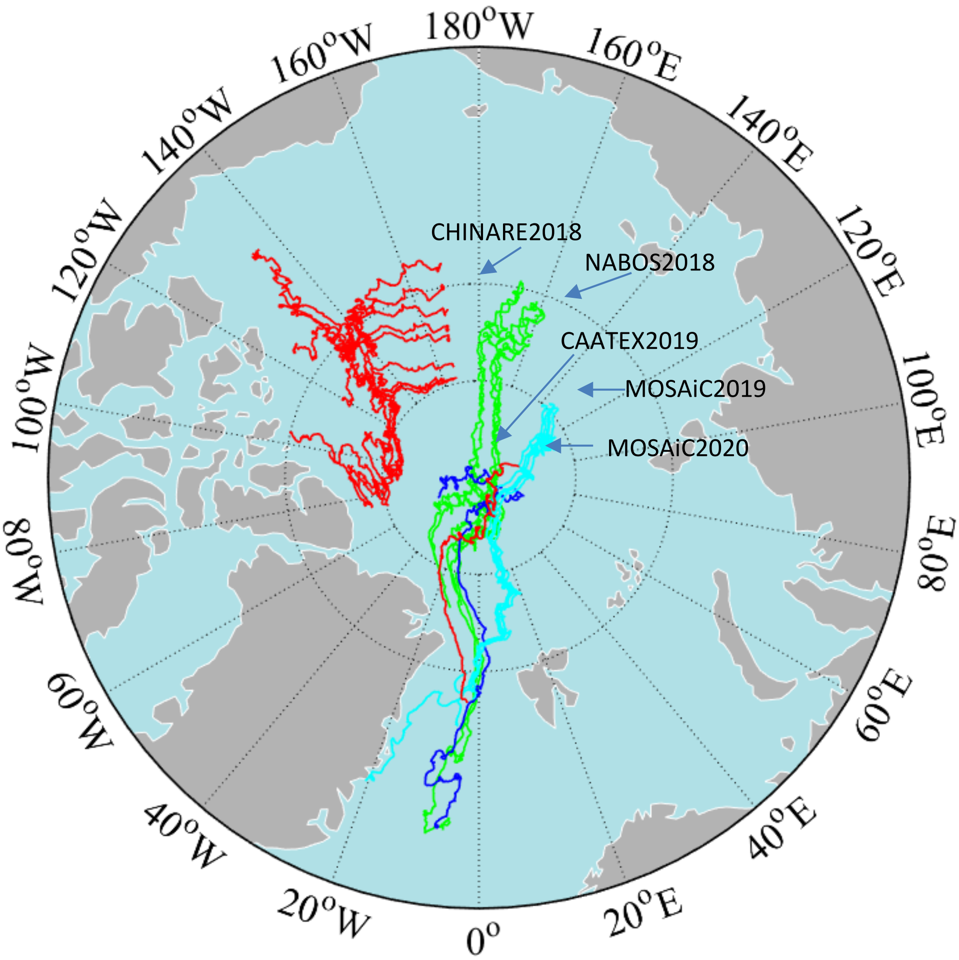


***Figure 2.2.1.*** *Trajectories of SIMBA buoys deployed in the Arctic in the period 2018-2020. Red: CHINARE2018 (11 buoys), green: NABOS2018 (5 buoys), blue: CAATEX2019 (2 buoys), light blue: MOSAiC2019 (leg1:15 buoys, not all of them are in the figure) and red in the central Arctic: MOASiC2020 (leg5: 4 buoys).*

*SIMBA2018*

Two major field campaigns were implemented in 2018. The Chinese Arctic Research Expedition program (CHINARE2018) was carried out in summer 2018. Eleven SIMBA buoys were deployed north of the Chukchi Sea in August by R/V Xuelong Chinese ice breaker (Fig. 2.2.2). The buoys drifted in the Pacific Arctic Section. The TRANSDRIFT/TICE/NABOS expedition was implemented by the Russia R/V Akademik Tryoshnikov in August 2018. Five SIMBA buoys were deployed in the Makarov Basin in September and drifted along the Transpolar Drift Stream toward the Fram Strait. Those SIMBAs worked reasonably well during the life spin time of about 1 year.


**Figure 2.2.2.** CHINARE2018 was implemented by R/V Xuelong ice breaker. The scientists are deploying SIMBA buoy on sea ice.

*SIMBA2019*

In 2019, 17 SIMBA buoys were deployed during two field programs. The CAATEX (Coordinated Arctic Acoustic Thermometry Experiment) research cruise was implemented by the Norwegian Coast Guard vessel KV Svalbard. Field experiments were conducted by Nansen Center in collaboration with eight other Norwegian and international research institutions. The vessel reached the north pole by the end of August and 2 SIMBAs were deployed and worked until February and July 2020, respectively. The major field campaign of the year was the MOSAiC2019 (Krumpen, et al., 2020). During the MOSAiC leg 1, 15 SIMBAs were deployed in the central MOSAiC ice camp and ice floes in the vicinity. These buoys covered a spatial scale of about 50 km.

*SIMBA2020*

MOSAiC leg 5 was implemented in 2020. Due to the fast drift of sea ice and weakening ice conditions, the MOSAiC leg 5 was not possible to work on the original MOSAiC ice floe. A number of new instruments have been installed on a new ice floe which was located close to the North Pole. Four SIMBA buoys have been deployed, 2 of them were INTAROS contribution. Those SIMBA worked until February and June 2021, respectively. The SIMBAs were deployed close to each other, but the ice conditions at deployment sites are different (Fig. 2.2.3). One SIMBA was deployed on level ice, another one was at a melt pond.

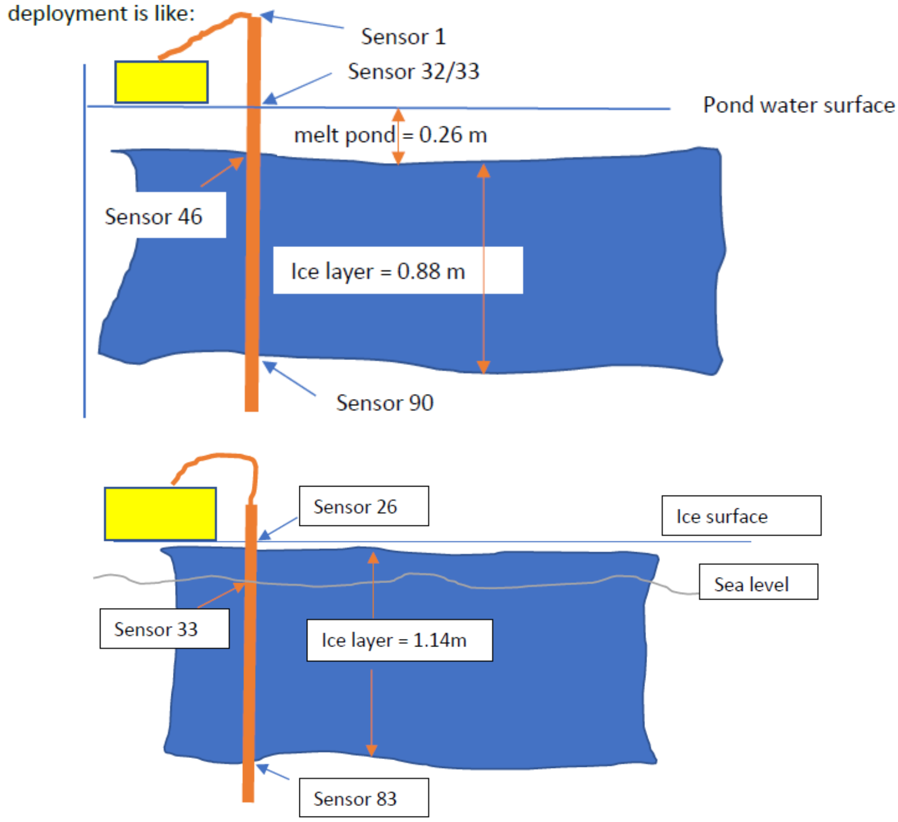


***Figure 2.2.3***. *Schematic illustration of SIMBA deployment during MOSAiC leg5. The thermistor string illustrated as orange bar was vertically placed through air-snow-sea ice- ocean.*

We need to emphasis that only partial SIMBA are funded by the INTAROS, the majority of the SIMBA were contributions from various research partners, thanks for the international collaborations.

In addition to those high profile large international field campaigns, small field programs have been organized during INTAROS period. One of such activity was carried out in the coastal land fast sea ice zone in the Young Sound, east Greenland. One SIMBA was deployed in October 2020 and worked until mid-April 2021.

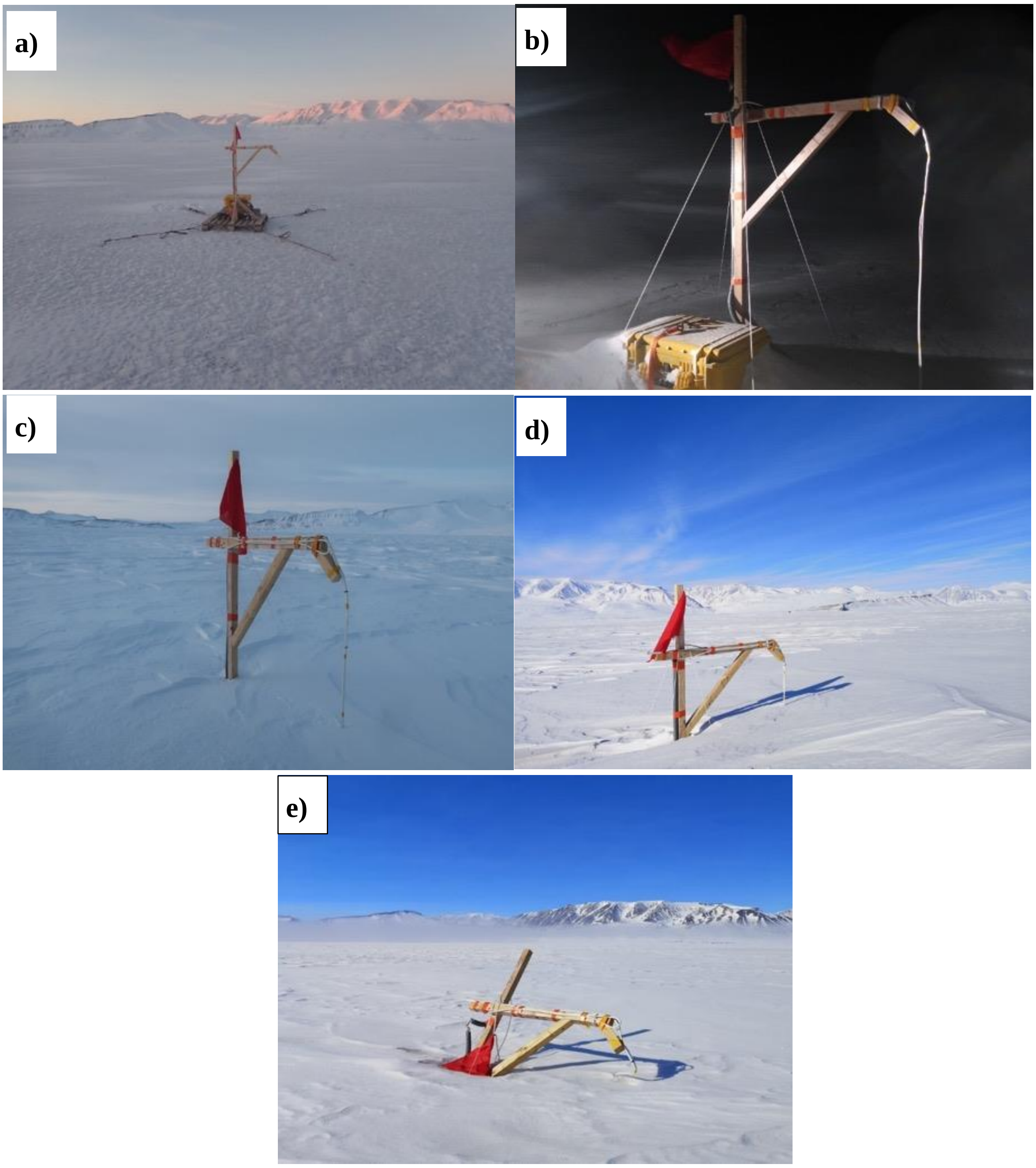


***Figure 2.2.4****. The SIMBA site at Young Sound east Greenland. A photo sequence of SIMBA during operation.*

Fig. 2.2.4 shows the evolution of the deployment site. The deployment was made by the Danish Navy on 28 October 2020 (Fig.2.2.4a). The surface was flat with a thin snow layer (0.5 – 1 cm). Ice thickness was 29cm. The air temperature was -10 °C during the deployment. The SIMBA site was visited by the Danish Navy personals and snow and ice thickness were measured. On 15 December 2020, the onsite snow depth was 26 cm. The snow was very hard and packed. The ice thickness was 47 cm (Fig. 2.2.4b). On 17 March 2021, the onsite snow depth was 79 cm. The snow was packed and hard. The ice thickness was 119 cm (Fig. 2.2.4c). During the measurement, the flooding was severe. This measurement created a massive slush formation. On 15 April 2021(Fig. 2.2.4d), the onsite snow depth was 72 cm. The snow was packed and hard. The ice thickness was 96 cm. The surface looked dry. But there was a deep slush layer between snow and sea ice. The SIMBA stopped working on 10 April. The possible cause could be flooding of the SIMBA Peli case or ice movement that damaged the thermistor chain. The slush layer was reported to be 60 cm. On 17 May 2021(Fig. 2.2.4e), it was clear that the ice below snow has moved so the SIMBA frame collapsed. The ice thickness was 114 cm, the dense slush/ice on top was 60 cm and the snow was 42 cm. Those onsite snow and ice survey and photos are very useful to validate SIMBA algorithm and to understand the possible cause of system failure technically and naturally.

All the SIMBA buoys deployed during INTAROS period have been terminated. Most of them worked quite well and provided valid observations data for scientific research (See section 2.2.3). Among all deployed SIMBAs, only few of them failed not long after deployment, mainly due to the malfunction of thermistor strings, probably caused by ice deformation.

### 2.2.2. Lessons learned and technology challenges identified during the project - SIMBA snow and ice mass balance buoys

SIMBA is clarified as the thermistor string-based ice mass balance buoy. A thermistor string is used to measure the environment temperature (SIMBA-ET) every 2 cm in a vertical length of 4.8m through air-snow-sea ice- ocean. Additionally, the thermistor chain is equipped with heaters. A weak voltage supply is connected to provide gentle identical heating of each sensor for a period of 60s and 90s to ensure heating temperature (SIMBA-HT) rise to reach a steady state. Thermal conductivity determines how the heat is conducted away of the heated sensors placed in air, snow, ice and lake water. As a result, the SIMBA-ET and SIMBA-HT profiles can detect and greatly enhance the identification of the interfaces between air, snow, ice and water. Several accessories equipped on SIMBA, e.g., built-in GPS to record SIMBA drift positions, a magnetometer for tilt and floe rotation, a barometer for surface air pressure, and an external sensor to measure near-surface ambient air temperature. An iridium modem is applied for data transmission. SIMBA has been used in various field campaigns targeting snow and ice mass balance in seasonally ice-covers in lakes (Cheng et al., 2014) and Polar Oceans (Hoppmann et al. 2015; Provost et al. 2017; Lei et al. 2018, 2021).

The biggest advantage of SIMBA is the cost-cutting design. In addition, SIMBA applied a simple deployment procedure and has the capacity to be recovered and reused multiple times. In Polar Oceans, especially Arctic, where sea ice drifts long distances and is under strong deformation, break up and leads open. The risk of losing expensive field equipment is high. The SIMBA cost cutting design can somehow minimize such risk economically. The spatial variations of snow and sea ice in the Arctic Ocean are large. A cluster-type of SIMBA deployments in regional domain could provide valuable in-situ data to extract better information on snow and ice temporal and spatial variations. This has been done already during the MOSAiC field campaign (Nicolaus, et al., 2021). So, SIMBA has been proved to be an adequate component of the Integrated Arctic Observation System.

However, there are still technical challenges to establish better SIMBA in situ configurations and to increase the liability and robustness of the of measurement during melting season. The thermistor string of SIMBA is deployed in a borehole of the ice floe. The borehole has to be refrozen entirely to ensure valid SIMBA data. On some occasions, as when SIMBA was deployed during summer, the borehole remains unfrozen for quite long time and could shorten time series of valid SIMBA data. The thermistor chain of SIMBA is vulnerable to the ice raft and deformation. It can also be damaged by the polar bears. During freezing season, sensors exposed in the air may suffer the impact of high-frequency variations, such as wind vibration, snow drift, frost condensation and lead to false temperature readings. During melting season, the absorbed solar radiation below ice surface can melt sea ice and create air bubbles and open space between thermistor sensors and surrounding ice resulting unexpected high temperature readings. A unified data processing technique to reliably and accurately determine sea ice thickness and snow depth from this kind of data is still missing, and an unambiguous interpretation remains a challenge. Several SIMBA algorithms have been developed (Zuo et al., 2018, Liao et al, 2018, Cheng et al, 2020) and worked well in cold condition. However, during summer melting season, the robustness of the algorithms reduced significantly. Further improvement of SIMBA algorithm in terms of fully utilize SIMBA-ET and SIMBA-HT data is underway.

The manual processing of SIMBA data is still largely used by individuals for research papers. In a long run, however, the SIMBA algorithm should be applied particularly for the operational analyses of SIMBA data in real time.

### 2.2.3. Description of processing and analysis of the obtained data - SIMBA snow and ice mass balance buoys

In addition to the GPS position (Fig. 2.2.1), time series of temperature (SIMBA-ET and SIMBA-HT) in air-snow-sea ice-ocean is the main output of SIMBA. The following Figs 2.2.5 and 2.2.6 show examples of SIMBA-ET and SIMBA-HT time series, respectively. We can see clearly during observation period, there were three major storm events. The air temperature increased between 20 – 30 degrees in a short period. We can see temperature in snow response strongly to these events. The temperature was observed by SIMBA 240 sensors mounted vertically in the air-snow-sea ice and water.

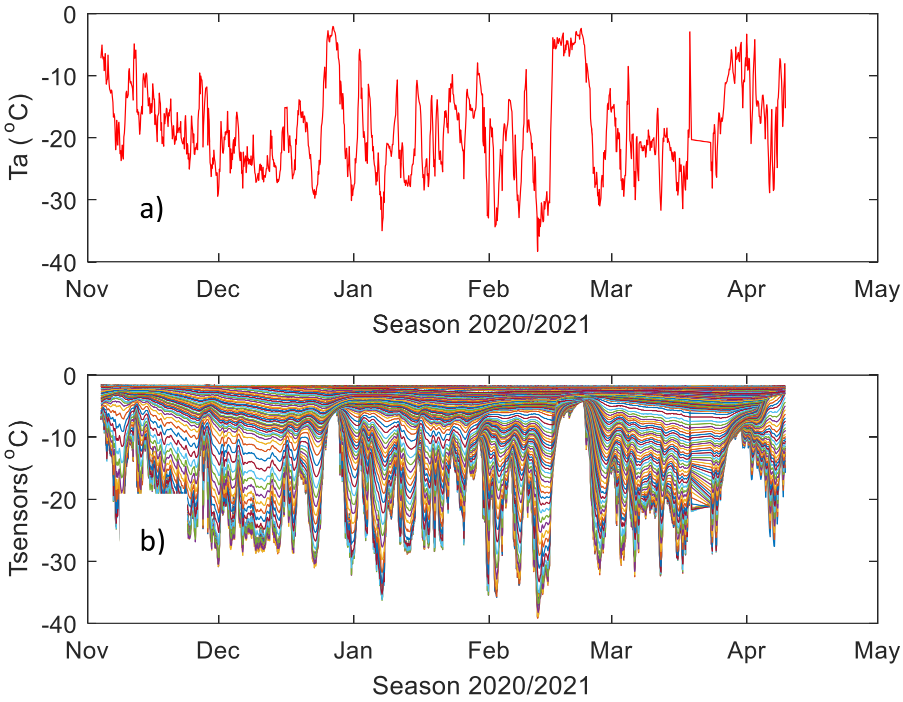


***Figure 2.2.5.*** *a) Time series of air temperature; b) Time series of SIMBA-ET. This SIMBA was deployed in Young Sound (Fig.2.2.4).*

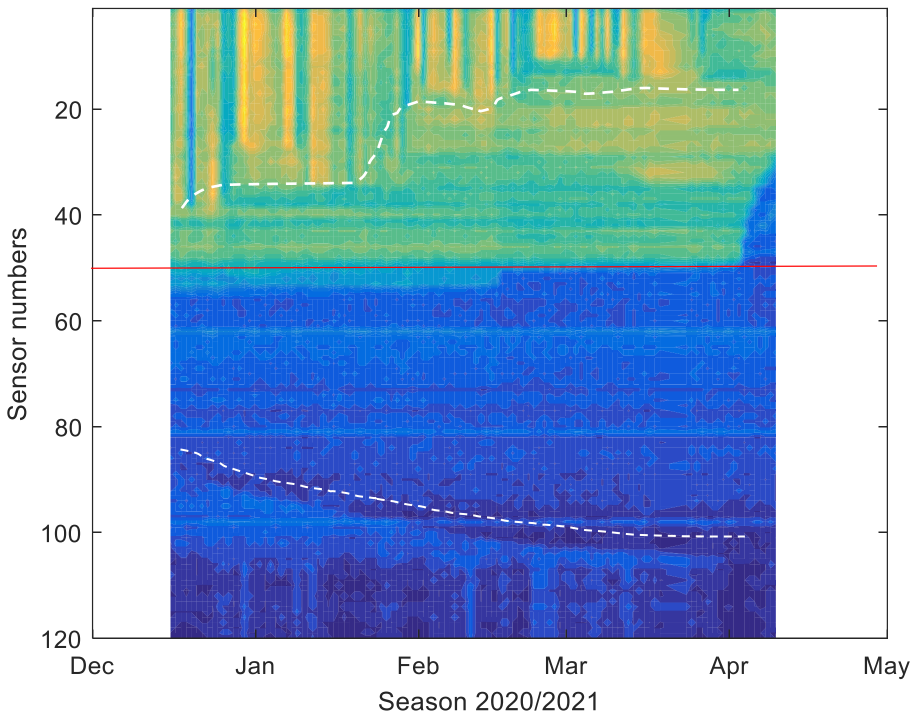


*Figure 2.2.6. The observed SIMBA-HT field. The red linen is the initial position of snow/ice interface. The white dashed lines are manually observed air/snow (top) and ice/ocean interfaces from which the snow depth and ice thickness can be obtained.*

The snow depth and ice thickness can also be retrieved by algorithm (e.g. Liao et al., 2019, Cheng et al., 2020). Fig. 2.2.7 shows one comparison where the snow depth and ice thickness are derived from SIMBA temperature fields both by manual and algorithm (Yong et al., 2021, submitted manuscript).

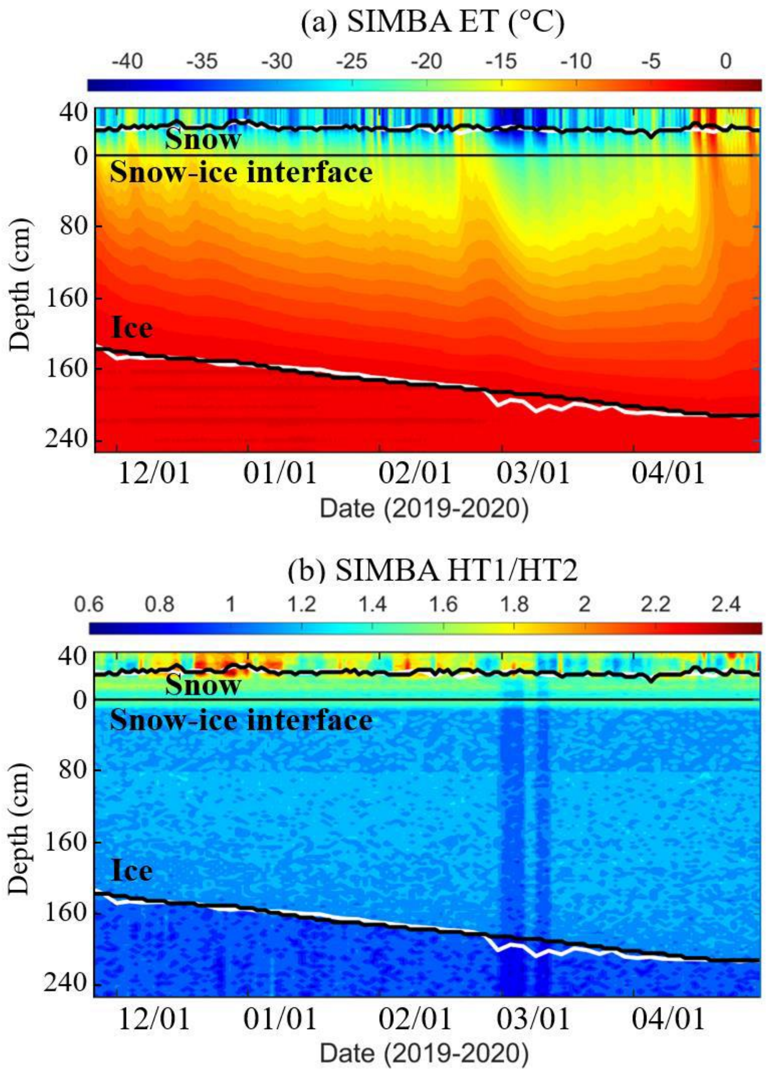


***Figure 2.2.7.*** *(a) Time series of the SIMBA-ET profiles. (b) Time series of the SIMBA-HT profiles. The white lines are results from the SIMBA algorithm and the black lines are results from the manual processing. This SIMBA was deployed during MOSAiC leg 1.*

So far, SIMBA algorithm mainly applies SIMBA-ET data to derive snow depth and ice thickness, SIMBA-ET is mainly used to validate algorithm results. However, SIMBA-HT can also be used to identify interfaces between air-snow-sea ice-ocean, in particular the ice-ocean interface. It is often visible from SIMBA-HT profiles. We are currently working on a procedure to identify ice-ocean interface applying neural networks (NEN), wavelet analyses (WAA) and Kalman filter (KAF). The procedure seems work well largely (Liao et al., 2021, under preparation). Fig. 2.2.8 shows a few examples of ice bottom detection using this procedure.

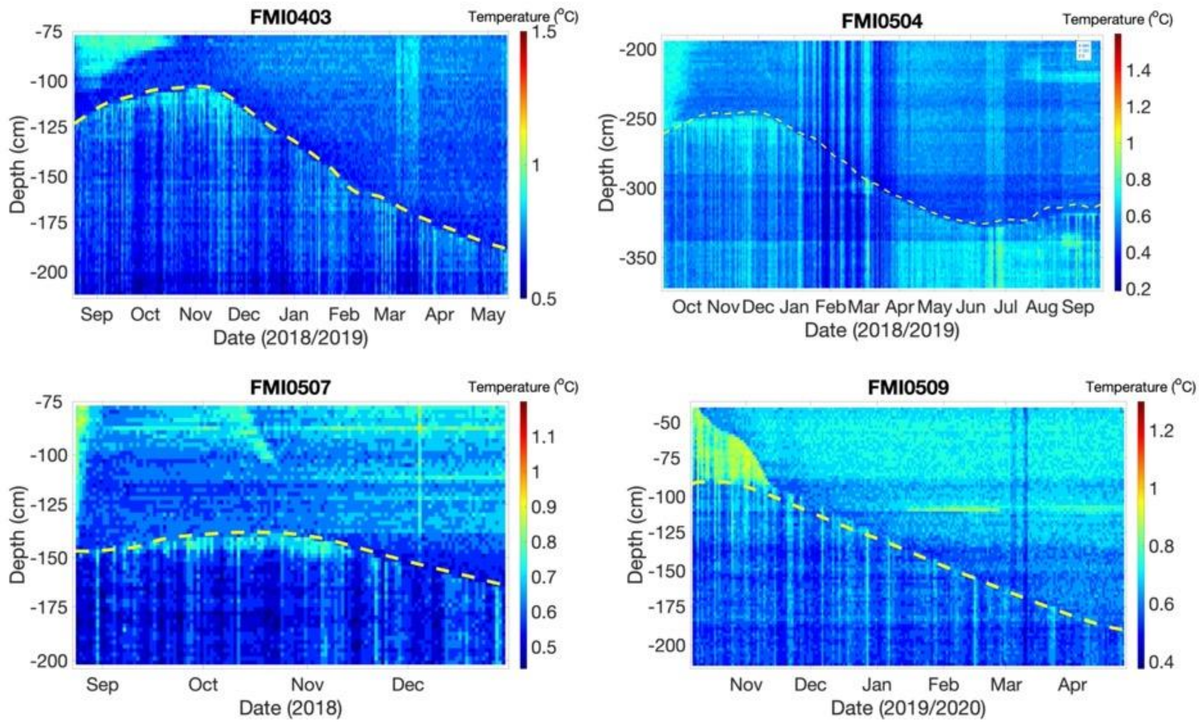


***Figure 2.2.8.*** *Several examples of SIMBA ice-ocean interface detection using SIMBA-HT based neural networks, wavelet analyses and Kalman filter integrated procedure. Those SIMBAs were deployed in the Arctic Ocean. The background are SIMBA-HT profiles. The dashed lines are detected ice bottom which agree well with the SIMBA-HT visualized ice-ocean interfaces.*

Another frontier on SIMBA algorithm development is to tackle the snow-ice interface detection. In conditions with a heavy snow precipitation falls on a thin ice layer, it may result in slush formation at the snow/ice interface and later in refreezing to snow-ice. Additionally, the snowmelt water, sleet and rain may refreeze to form meteoric ice at the snow/ice interface. Hence, the snow/ice interface is a dynamic moving boundary between the snow cover and underneath ice floe (Cheng et al., 2014). These conditions are largely occurred in the boreal lakes. However, under climate change, the Arctic sea-ice thickness is decreasing, and snow depth is increasing. Snow-ice formation observed in the Arctic winter has resulted in snow/ice interface moving upward (Provost et al., 2017). Therefore, it is necessary to develop such algorithm. One study has been carried out focusing on SIMBA lake data processing (Cheng et al., 2020). The new algorithm has been used to process data obtained from a sustainable SIMBA lake program which has been so far lasted for a decade and will continue in the future (Cheng et al., 2021). This SIMBA lake program is a spin-off of INTAROS SIMBA activities.

In addition to systematic SIMBA data analyses and algorithm development summarized above, individual scientific papers have been produced and under constructions applying SIMBA data. A study has been published on investigation of the seasonal changes in sea ice kinematics and deformation apply SIMBA drift data (GSP) along with drift buoy data (Lei, et al., 2021). The study focused on ice dynamics in the Pacific Arctic Region. The SIMBAs deployed during MOSAiC leg 1 have been used to estimate the dynamic and thermodynamic contributions on sea ice growth in connection with remote sensing ICESat-2 data (Yong et al., 2021, submitted) and applied for seasonal evolution of the sea ice thickness distribution in the Transpolar Drift (Albedyll, et al, 2021, to be submitted to TC). A comprehensive investigation on seasonality of thermodynamic mass balance and heat fluxes of the Arctic Sea ice during MOSAiC Transpolar Drift in 2019/20 is under final preparation (Lei et al., 2021, to be submitted to Elementa). The SIMBA data obtained from MOSAiC leg 5 are used to elevation difference between CryoSat-2 (Ku-band) and IceSat-2 (Laser) within the framework of the CRYO2ICE. The modelling of snow and sea ice mass balance is underway along SIMBA drift trajectories for better understanding the effect of atmosphere and ocean on sea ice during extreme, such as storm events.

### 2.2.4. Accessibility of the obtained data sets and repositories used - SIMBA snow and ice mass balance buoys

The original SIMBA data, i.e., time series of the SIMBA-ET, SIMBA-HT, GPS position were archived in the data server of the SIMBA manufacturer SAMS under secured password required weblink for each customer. Some of the SIMBAs deployed, e.g., during NABOS and MOSAiC were processed and archived at https://www.meereisportal.de/. Due to different data policy of different international Arctic field expeditions, it is not possibly yet to establish any universal SIMBA data platform. However, several INTAROS partners (FMI, PRIC and NMEFC) have agreed to accesses and share their SAMS SIMBA customer data webpage.  The SIMBA deployed by those partners will be registered in the INTAROS Data Catalog https://catalog-intaros.nersc.no/

The SIMBA raw data are standard excel sheets files. The SIMBA-ET and SIMBA-HT are temperature data in Celsius degree and GPS position are digitized as lat/lon numbers with 5 decimals. The accuracy of SIMBA temperature sensor and GPS position were ± 0.1 ºC and 2m, respectively.

We are currently working on upload of the SIMBA data into https://zenodo.org/deposit. Arctic lake SIMBA observation data set to be act as a spin-off and parallel to the INTAROS SIMBA activity has been registered in the Zenodo:
https://zenodo.org/record/4559368#.YIKOOpAzZPZ (Cheng et al, 2021). Similar work is under construction to archive for Arctic SIMBA data.

The SIMBA data registered in the INTAROS Data Catalog https://catalog-intaros.nersc.no/ will be freely available for the society.

### 2.2.5. Future plans for operation of the observing system, including data provision - SIMBA snow and ice mass balance buoys

It seems no major international Arctic field campaign will take place in the near future. However, some small-scale Arctic field program have been planned. The Young Sound SIMBA deployment will be carried in late autumn 2021. We plan to deploy one SIMBA together with several underwater instrument (measuring light, salinity, temperature, etc.). A digital camera system will be installed on land taking daily images. Several land-based weather stations measure energy flux, temperature, and snow metrics on land (coverage, melt and thickness). This field work in coordinated by the Arctic Research Centre (ARC), Aarhus University, Denmark.

A scientific research cruise will be organized by the Nansen Environmental and Remote Sensing Center (NERSC). The cruise starts from Tomrefjord in Norway on 27 August and ends in Tromsø on September 15, 2021. Two SIMBA buoys will be deployed in the central Arctic, preferably in the North Pole. The SIMBA buoys are in-kind contributions from FMI.

SIMBA has been previously deployed outside Bolshevik Island in Russia Arctic as part of Finnish-Russia collaborations under the umbrella of the Pan-Eurasian Experiment (PEEX) program. There have been discussions to continue SIMBA measurement as expansion of the PEEX marine component. The SIMBA measurement maybe established at new Russia polar station at Severnaya Zemlya.

In addition to various SIMBA deployment in the Arctic Ocean. The FMI has operated a long-term sustainable Arctic Lake SIMBA program in the Finnish Lapland. We deployed one SIMBA in lake Orajärvi every winter season since 2009. The data has been used to develop SIMBA algorithm (Cheng et al., 2020) and to study snow and ice interactions. This SIMBA program can be regarded as a spin-off of INTAROS SIMBA activity. We have published a data paper in ESSD (Cheng et al., 2021).

The CHINARE program as well as AWI's TRANSDRIFT/TICE cruise are sustainable Arctic expedition platforms that can be used for SIMBA deployment in the future.

*Data exploitation.* During INTAROS period, at least 38 SIMBA ice mass balance buoys have been deployed in the Arctic Ocean. This achievement is almost 3 times more than INTAROS has promised.  SIMBA system is proved to be a reliable and robust observation platform. Several studies based on SIMBA data have been carried out and some more are still coming. The topics are focused on snow and ice physics, seasonal dynamics and thermodynamics, as well as remote sensing and processing modelling.

### 2.2.6. Results of the final implementation of the observing system - Fixed station and UAV-based radiation measurements during the MOSAiC expedition

The FMI broadband radiation station was installed on the main ice floe of the MOSAiC experiment from November 2019 until November 2020 (Fig. 2.2.9). The station includes upward and downward facing pyranometers and pyrgeometers to measure the surface shortwave and longwave radiative budgets, as well as an upward facing SPN1 sunshine pyranometer to measure the diffuse global radiation. The station is complementary to other similar stations installed on different surface types (first- and second-year ice, melt ponds, ridges, leads) to observe the surface yearly evolution of the sea ice surface radiation budget.

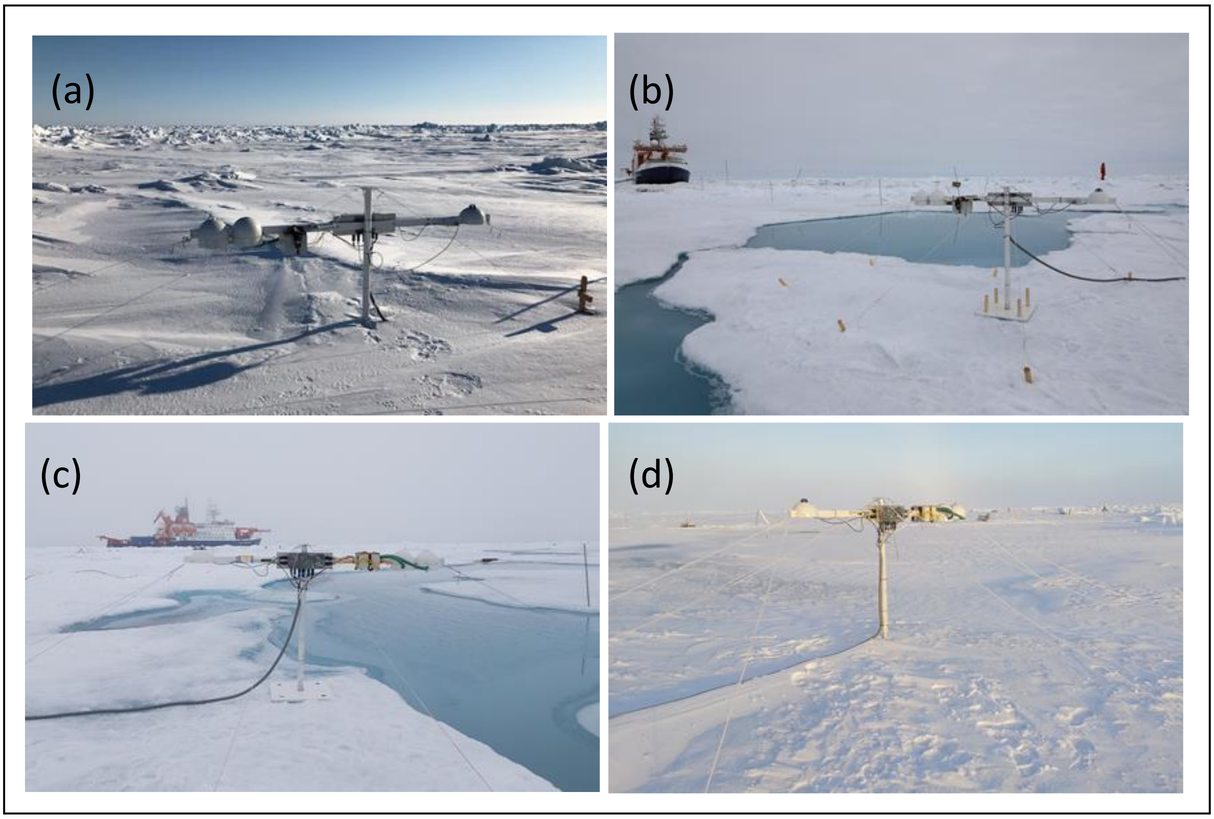


*Figure 2.2.9. FMI broadband radiation station installed on the main ice floe of the MOSAiC experiment during leg 1-3 (a, Photo: C. Cox), leg 4 (b, Photo: M. Shupe), and leg 5 (c and d, Photos: R. Pirazzini). The station remained in the same position during legs 1-3, it was moved in a new position during leg 4, after the ship Polarstern returned to the original ice floe, and it was placed in a new ice floe during leg 5, after the original ice floe disintegrated. A remarkable change in surface properties occurred during leg 5 when the initial open melt ponds (c) froze and were covered by new snow (d).*

Preliminary results show that the changes in surface properties are well reflected by the time series of the measured surface albedo (Fig. 2.2.10), with initial values above 0.8, typical of dry snow, lower values (around 0.6) during the summer melting in proximity of a melt pond, decreasing as the increase of the melt pond.

During leg 5 the pyranometers were placed above a melt pond (Fig 2.2.9c): the albedo was around 0.3 at the beginning, when the pond was still widening, and in one week it increased up to 0.9 because of melt pond freezing and snow falling. The following rain and melting caused a ~20% albedo decrease on 13 and 14th of September, to finally reach the winter value around 0.8.

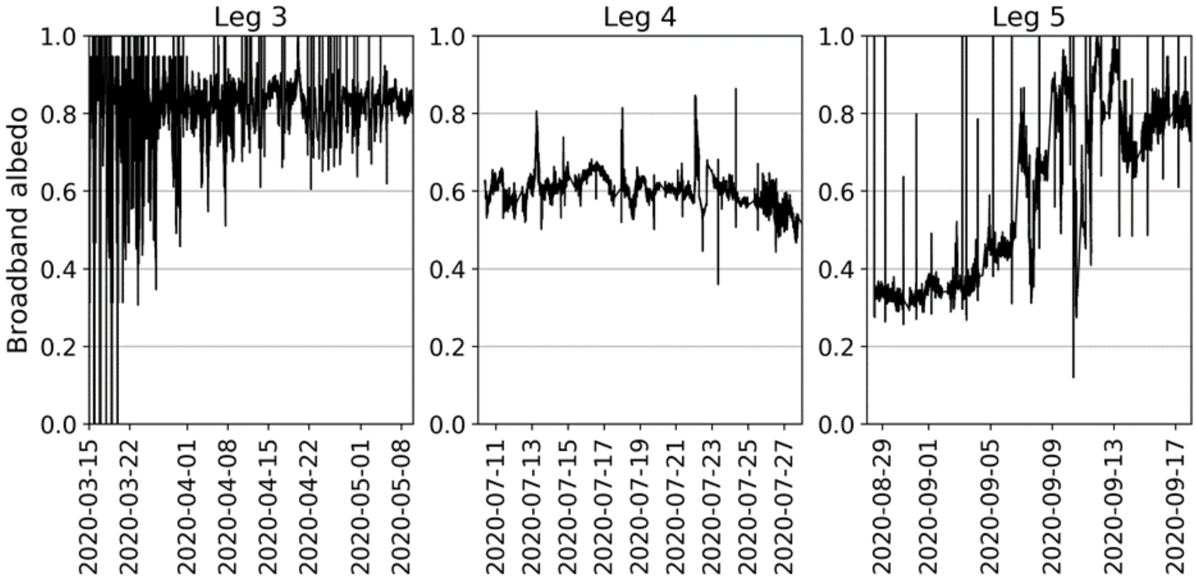


***Figure 2.2.10.*** *Surface albedo measured at the FMI broadband radiation station from 15.03.2020 until 18.09.2020.*

During MOSAiC leg 5 the drone SPECTRA equipped with broadband and spectral radiometers (Fig. 2.2.11a) was operated in synergy with a smaller drone (Mavic 2 Pro, Fig. 2.2.11b) equipped with camera to perform photography mapping of the area measured by the SPECTRA drone.

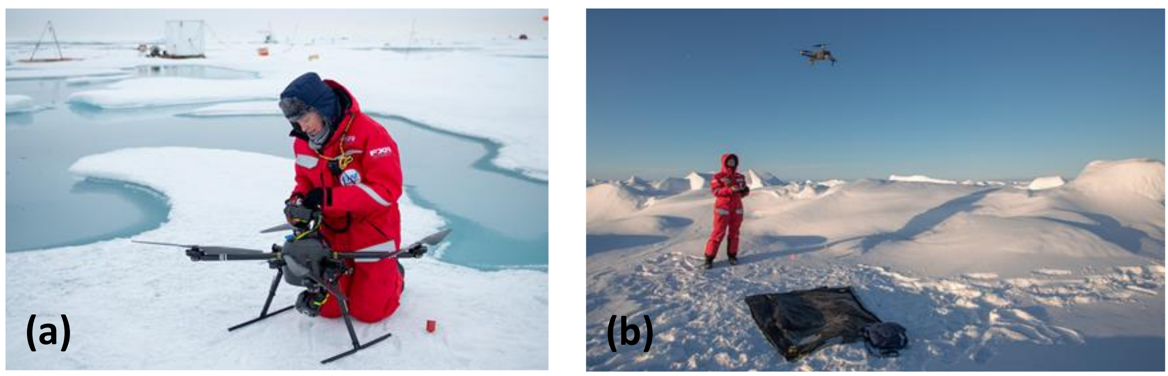


*Figure 2.2.11. SECTRA drone equipped with upward and downward looking broadband and spectral radiometers (a, Photo: J. Rohde) and Mavic 2 Pro drone equipped with camera (b, Photo: L. Nixon).*

First, a photography mapping of the target area from an altitude of 40/50 m was performed with Mavic 2 Pro while the instruments of the SPECTRA drone were running to reach the thermal equilibrium with the ambient temperature. Then, if the Mavic drone did not experience icing on the propellers and thus did not activate a forced landing, the SPECTRA drone was operated for up to three consecutive flights, each of them lasting approximately 20 minutes. The Mavic 2 Pro drone was guided along a serpentine pattern to reach a high overlap (ideally about 80%) between the photos and, thus, enable the derivation of the 3D surface topography through image processing. The SPECTRA drone was mostly guided along repeated transects at 5 m, 10 m, and 30 m elevations. Vertical profiles of albedo with SPECTRA hovering for 1-2 minutes at 5 m, 10 m, and 30 m were repeatedly carried out at specific locations over flags or buoys. Figure 2.2.12 show the location of the flight areas in the MOSAiC drifting ice floe: yellow lines correspond to the paths of the Mavic 2 Pro drone, yellow crosses being the starting point of the flights, while red dotted lines correspond to the transects measured with SPECTRA drone. The red dots mark the location of the vertical profiles made with SPECTRA. Altogether, 17 flights were carried out with SPECTRA for 8 days, corresponding to ~5 flight hours, and 35 flights with Mavic 2 Pro during 18 days, corresponding to ~11.5 flight hours.

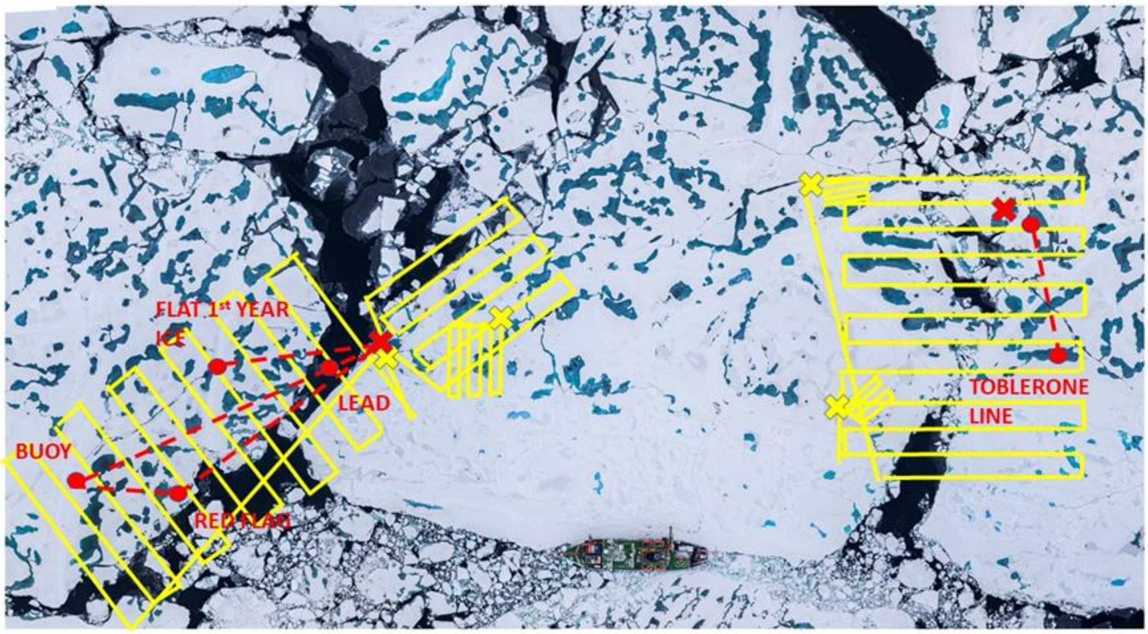


*Figure 2.2.12. Location of the flight areas in the MOSAiC drifting ice floe (underlying Photo-mosaic: S. Graupner): yellow lines correspond to the paths of the Mavic 2 Pro drone, while red dotted lines correspond to the transects measured with SPECTRA drone. The red dots mark the location of the vertical profiles made with SPECTRA.*

From a very preliminary look into some of the collected data (Fig. 2.2.13) it appears that areal-averaged albedos measured at the elevation of 5m and 10m above sea level have a larger variability than the areal-averaged albedo measured at the elevation of 30m (red lines in Figure 2.2.13). A certain degree of albedo variability is unavoidable even during hovering at 30m because it is not possible to keep the drone over the same surface while the ice is drifting. However, the fact that on 1st and 4th of September the 30m albedo was similar even over different targets may suggest that the 30m albedo is not significantly affected by the individual surface features and, therefore, it is potentially representative for satellite footprint and model grid area. It is also worth noticing that the 30m albedo measured on 1st and 4th of September was around 0.4, consistently with the averaged albedo value measured along the Kinder line in the same period.

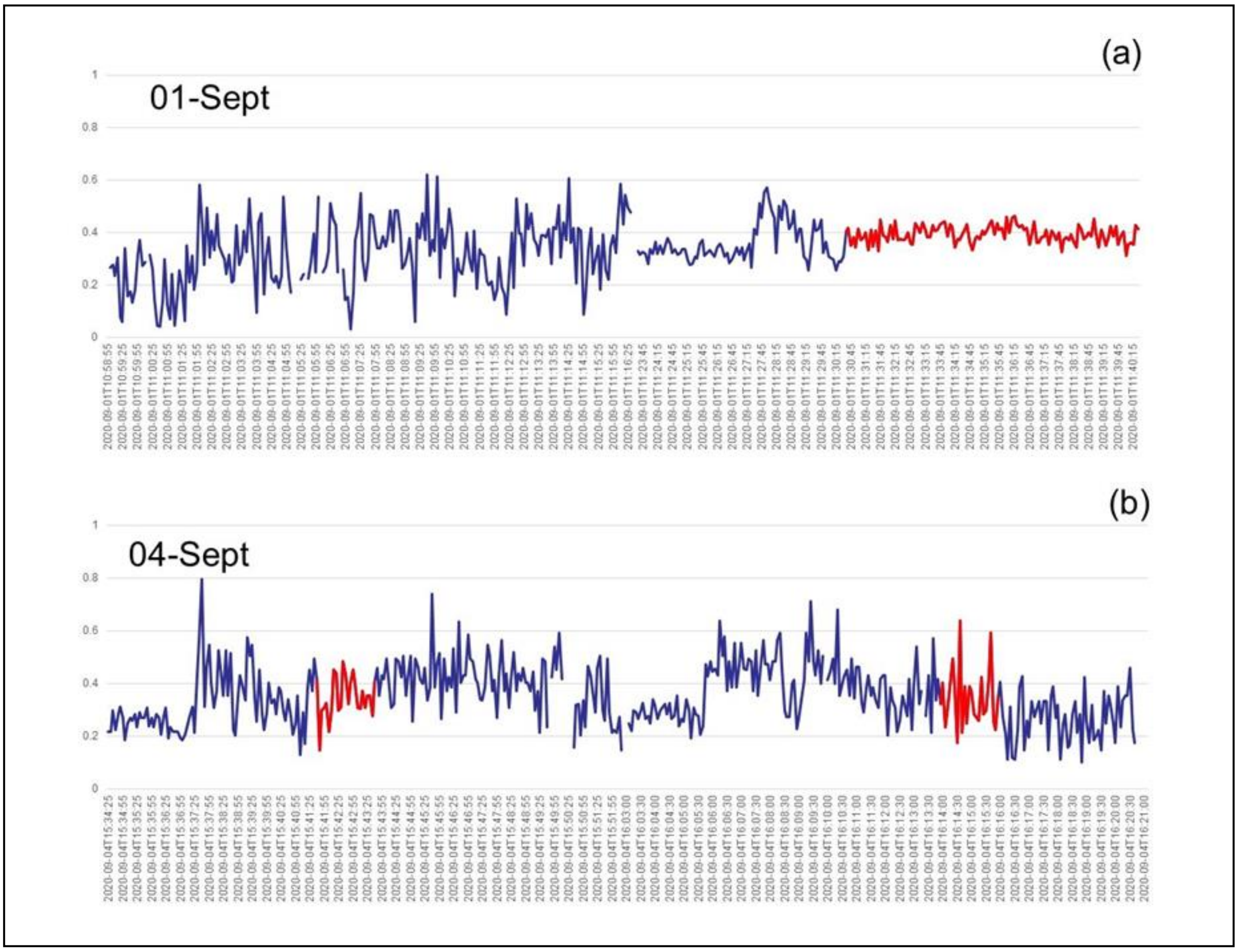


*Figure 2.2.13. Time series of broadband albedo measured with SPECTRA during selected flights on 1st of September (a) and on 4th of September (b). Red lines correspond to albedo measured at 30m above sea level.*

### 2.2.7. Lessons learned and technology challenges identified during the project - Fixed station and UAV-based radiation measurements during the MOSAiC expedition

Concerning the FMI fixed radiation station, the secondary electrical circuit developed to guarantee power supply when the main power line breaks for few days proved to be successful: the station never experienced power breaks, also thanks to the metal tubes protecting the electrical cables against the bites of polar foxes and bears. However, the domes of the upward looking pyranometers needed to be cleaned from condensation or brine/ice formation on daily basis, in some cases even several times per day, as the applied ventilation system was insufficient to keep the domes cleaned and dry (Fig. 2.2.14a).

Drones proved to be extremely valuable tools to measure the surface albedo over sea ice, as they enable the characterization of the heterogeneity of the surface and the area-averaged measurement of the radiation fluxes. However, many challenges were faced when operating the drones: the moist and freezing air conditions often prevented the flights, as ice quickly formed on the propellers (Fig. 2.2.14b). Moreover, the proximity with the geographical North Pole made the navigation systems very unreliable and unstable, especially in the case of the big SPECTRA drone that has a relatively big inertia, and it requires more time to correct unexpected drifts. Therefore, take-off, landing, and part of the flights with SPECTRA were carried out in manual mode, without GPS positioning, and compass driven mode was switched on/off several times until SPECTRA was stable enough also in the compass-driven mode.

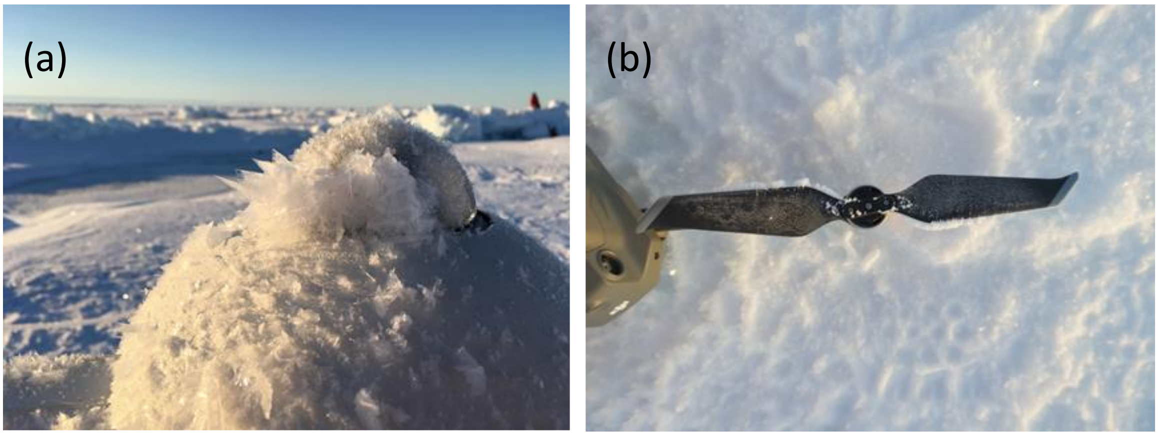


***Figure 2.2.14.*** *Frost formed on the dome of the upward looking pyranometer in the FMI radiation station ((a, Photo: Z. Brasseur) and at the front edges of the Mavic 2 Pro propellers (b, Photo: R. Pirazzini) on 11th of September.*

The detachment of the target area from the main floe made it difficult to repeat the flights over the same targets (distances from the starting point were changing, and sometimes the targets were hardly visible), and the drift of the ice floe during the flights required continuous adjustments of the loitering positions (in the case of SPECTRA) and of the lateral shifts in the serpentine pattern (in the case of Mavic 2 Pro). When temperatures dropped below -5°C it became difficult to keep the fingers warm and able to operate the sticks of the radio-controller for 20 consecutive minutes. Finally, the solar elevation decreased throughout the observing period, with a consequent decrease in the signal to noise ratio in the broadband radiation measurements and an increase of the integration time in spectral irradiance measurements. The SPECTRA drone was therefore not operated after 12th of September, when solar elevation did not exceed 5 degrees.

### 2.2.8. Description of processing and analysis of the obtained data - Fixed station and UAV-based radiation measurements during the MOSAiC expedition

All the radiation sensors installed in the fixed station and in the drone, SPECTRA were calibrated before and after the expedition. In addition, thermal and angular characterization of the broadband and spectral shortwave radiometers were performed in the FMI optical laboratory, to better assess the measurement uncertainty and correct for errors introduced by thermal drift of the sensor's sensitivity and deviation from perfect cosine response. The cleaning of the data from the erroneous values obtained when frost formed on the dome of the sensors is undergoing. The data correction and cleaning will be the first steps of the data processing, needed for the publication of the data.

### 2.2.9. Accessibility of the obtained data sets and repositories used - Fixed station and UAV-based radiation measurements during the MOSAiC expedition

All final data (broadband longwave and shortwave fluxes, broadband and spectral albedo, surface maps obtained from drone-based photo-mosaics) will be stored at the MOSAiC Central Storage (MCS) and at PANGAEA (World Data Center PANGAEA Data Publisher for Earth & Environmental Science (www.pangaea.de)) after post-processing and quality checks. Storage and release of data follow the MOSAiC data policy. All data will be handled, documented, archived and published following the MOSAiC open data policy.

### 2.2.10. Future plans for operation of the observing system, including data provision - Fixed station and UAV-based radiation measurements during the MOSAiC expedition

The fixed-position and drone platforms are developed to be used over sea ice during research cruises or during coastal-based field campaigns. They will be used in other ship of opportunity that go to the Arctic and in the upcoming sea ice campaigns where FMI personnel will participate.

*Data exploitation.* The collected data will be exploited first be the MOSAiC community, and later by the public. Surface radiation budget data from the FMI broadband radiation station complement those collected in other areas of the ice flow. They will be applied to study all physical and biological processes in the atmosphere, ice, and ocean that are driven by solar and thermal radiation. Data collected when the MOSAiC ice floe reached the lowest latitudes (north of Svalbard) will be applied for validation of satellite optical products. Airborne albedo and photogrammetry data collected with the drones are used to study the horizontal variability of albedo and surface roughness at different scales. This has application in the assessment of spatial representativeness of fixed surface radiation stations, and in sea ice albedo and radiative transfer modelling.

## 2.3. NIVA – new sensors and samplers for FerryBox system

Contributors: Andrew King, Kai Sørensen, Bert van Bavel, Sabine Marty, Pierre Jaccard, Marit Norli, Elizaveta Protsenko.

### 2.3.1. Results of the final implementation of the observing system

NIVA's contribution to Task 3.4 included the implementation of three different types of sampler/sensors on the Barents Sea Opening FerryBox system that operates between Tromsø, Norway and Longyearbyen, Svalbard on the container ship M/S *Norbjørn* (Fig. 2.3.1). The three instruments include a microplastics sampler, a combined deployment of spectrophotometric sensors for measuring pH and $CO_3$ ion, and an integrated sphere absorption meter sensor for measuring optical properties of seawater including dissolved organic matter and phytoplankton chlorophyll-a and taxon-specific pigments.

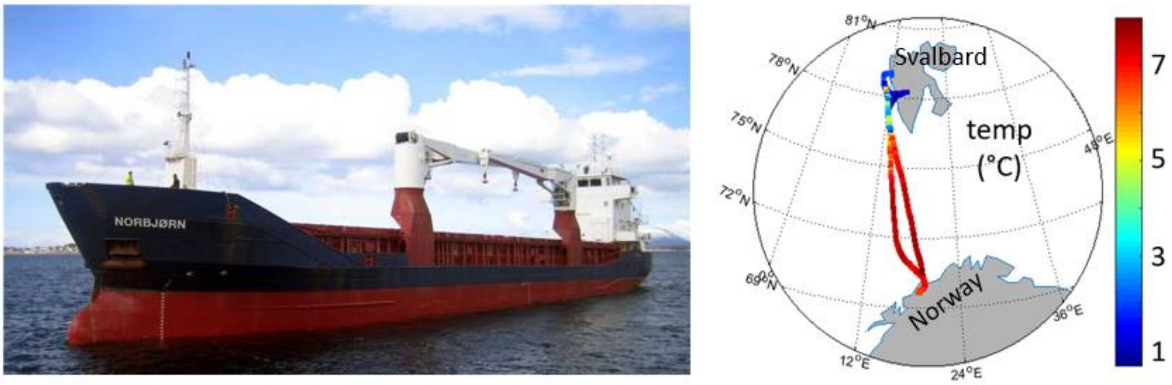


***Figure 2.3.1.*** *Photo of the Barents Sea Opening FerryBox ship of opportunity M/S Norbjørn (left) and typical route between Tromsø, Norway and Longyearbyen, Svalbard with example sea temperature data (right).*

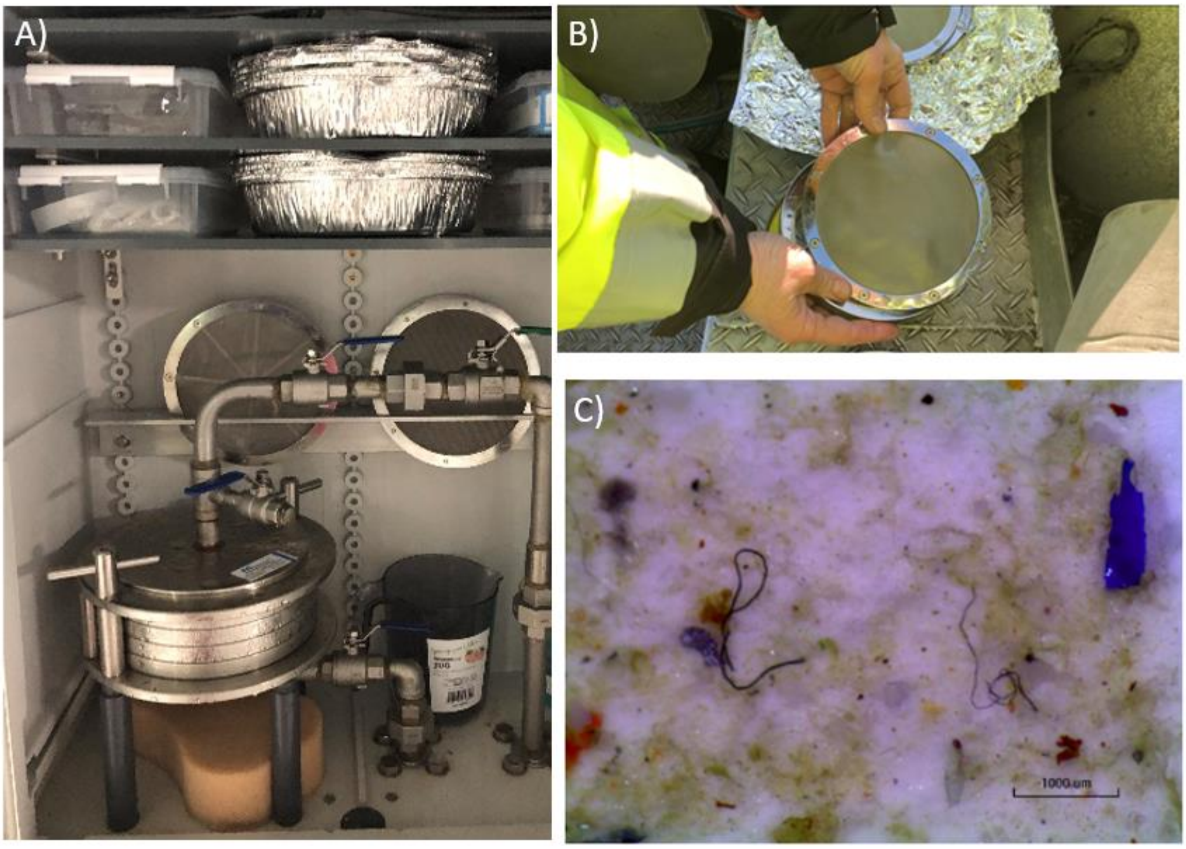


***Figure 2.3.2****. A) Photo of the INTAROS microplastics sampler equipped with three stacked filters in a dedicated FerryBox cabinet; B) Photo of a stainless steel filter (view from top) used to collect microplastics; C) Example of biological and abiotic material collected by the microplastics sampler; scale bar = 1000 µm.*

For the first activity, a microplastics sampler was constructed and developed for automated operation alongside a FerryBox sensor system and deployed in the Barents Sea Opening. The sampler is fully non-plastic and can hold three stainless steel filters (~30 cm in diameter) with size cutoffs at 500, 300, and 100 (or optionally 50) µm (Fig. 2.3.2). Since microplastic particles are typically present at ~1-10 per m$^3$ in seawater (Lusher et al., 2015), a relatively large volume of seawater (>10,000 L) is required to get statistically significant quantities of particles. Therefore, a dedicated centrifugal pump (Iwaki Nordic A/S) was used that can pump upwards 900 L of seawater per hour through the filters, and flow rate is precisely measured using a digital flow meter.

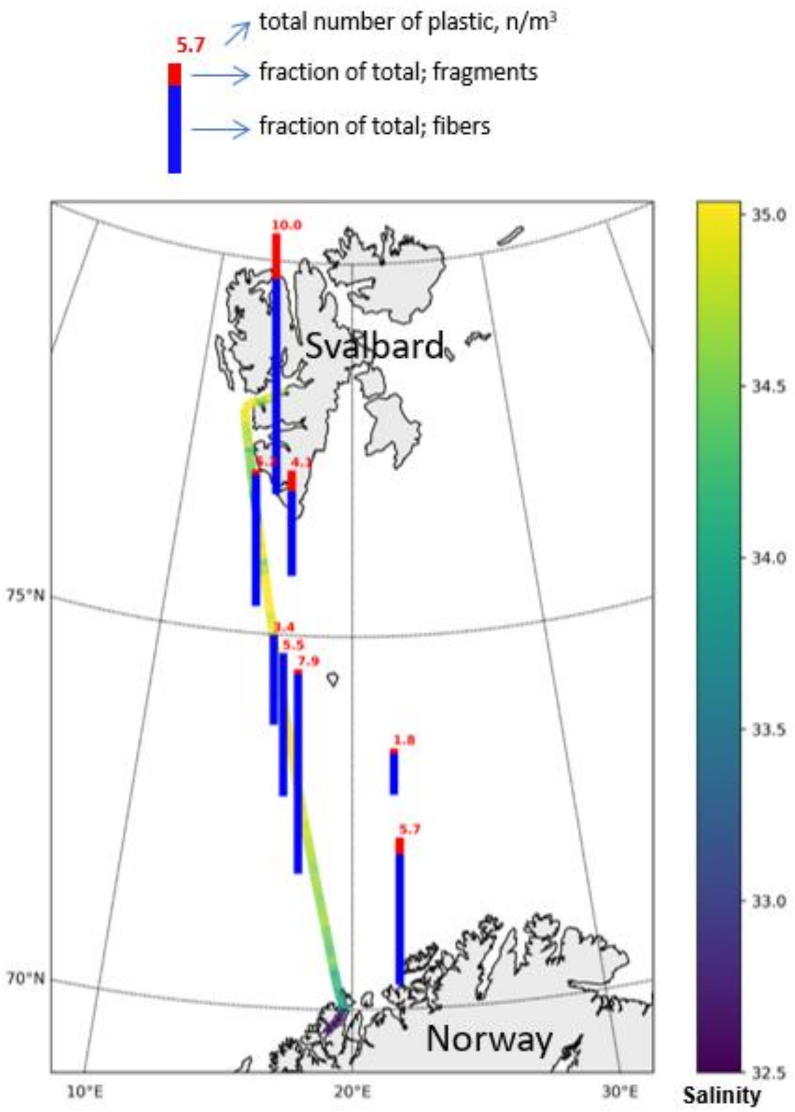


***Figure 2.3.3.*** *Concentration of microplastics collected during field campaigns in spring and summer 2019 in the Barents Sea Opening. Each sample consisted of filtering over 1000 L of seawater. The total number of plastic particles is shown in the red number on top of each bar, the red portion of the bar represents the fraction of total particles that is composed of fragments, and the blue part of the bar represents the fraction of total particles that is composed of fibers. A typical spring/summer salinity transect is also shown.*

In 2019, the microplastics sampler was deployed in the Barents Sea Opening where microplastics were collected from several transects between Tromsø, Norway and Ny Ålesund, Svalbard. The samples were processed and analyzed in the lab which included digestion of biological material (phytoplankton and zooplankton) and analysis by microscopy and Fourier-transform infrared spectroscopy for plastic type. Microplastic fragments/particles and fibers were present at all sampling points across the Barents Sea Opening. The concentration of total microplastics was ~2-10 per $m^3$ seawater, with ~0.1-1.8 per $m^3$ seawater accounted for by fragments and the remainder and majority as fibers (Fig. 2.3.3). The highest concentrations of fragments were observed near the Norwegian and Svalbard coast. This is in line with the higher levels of human activity and sources of plastics in coastal regions.

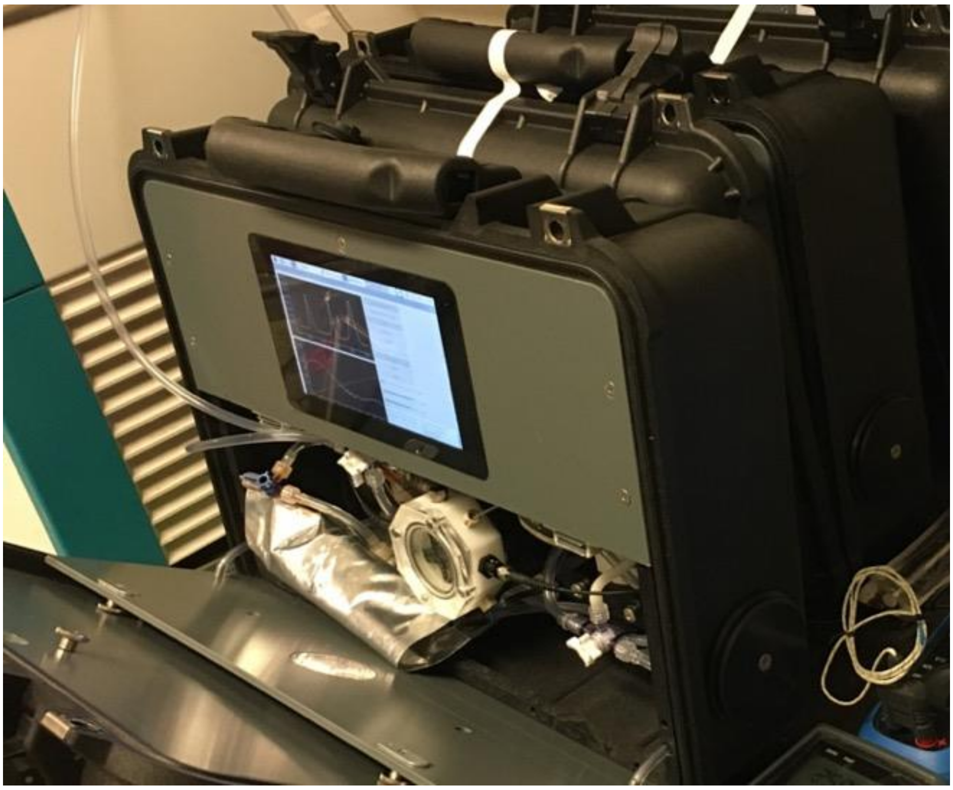

***Figure 2.3.4.*** *A photo of the spectrophotometric pH sensor system that is designed to operate on a FerryBox combined with a spectrophotometric $CO_3$ ion sensor system. It is designed to fit in a Pelicase (model 1500) for easy transportation and modular installation. Seawater is pumped into the analytical cuvette (white hexagon below touchscreen), flow is stopped, pH indicator reagent m-cresol purple is added (stored in the gas-tight foil bag), and absorbance is measured using LED light sources and an Ocean Insight STS-VIS spectrophotometer. A touchscreen is integrated with the sensor that allows for both control and visualization of data via a Raspberry pi/Python GUI. The two plots that can be seen on the left side of the touchscreen show light intensities provided by the LED sources (top plot) and absorbance calculated from the change in intensities after indicator addition (bottom plot).*

The second activity involved developing a combined spectrophotometric pH/$CO_3$ system which was field-tested in 2018 and further refined in 2019 and 2020 and deployed on the Barents Sea Opening FerryBox in 2020 and 2021. The sensor for measuring pH via spectrophotometry and indicator dye m-cresol purple (Fig. 2.3.4) was deployed on the Barents Sea Opening FerryBox from May 2020 to August 2021 (Fig. 2.3.5), however the FerryBox system was offline for equipment upgrade during the period between December 2020 and April 2021. The sensor for measuring $CO_3$ ion concentration via UV-VIS spectrophotometry took longer to develop and was delayed due to signal instability and high signal-to-noise ratio in the UV wavelengths of interest (234 and 250 nm). After testing two miniature UV-VIS spectrophotometers (Mightex HRS-UV1 and Ocean Insight STS-UV), it was determined that neither spectrophotometer was fit-for-purpose in terms of sensitivity and stability at the ~234-250 nm range. After further consultation and testing, an Ocean Insight FLAME-T-XR1-ES was found to have a sufficient level of stability and signal-to-noise, and this spectrophotometer was ultimately selected and integrated into the $CO_3$ sensor system. For the UV light source, a Heraeus FiberLight D2 HighPower Deuterium light source was integrated into the sensor system. The $CO_3$ ion system (Fig. 2.3.6) was installed on the Barents Sea Opening FerryBox in April 2021, but the system is not fully operational due to pump and flow issues. Preliminary data showing $fCO_2$ (µatm), pH (total scale), and $CO_3$ ion (µmol kg-1) for a transect from Tromsø-Longyearbyen between 13-18 August 2021 is shown in Fig. 2.3.7. The pH/$CO_3$ sensor system suffered from delays due to COVID-19 with respect to delayed development, fabrication, installation, maintenance, and calibration of equipment due to limited access to the lab, limited access to the FerryBox system related to travel restrictions, ship company boarding restrictions, and limited personnel capacity. There were also delays in receiving equipment from the spectrophotometer supplier due to reduced operations during COVID-19.

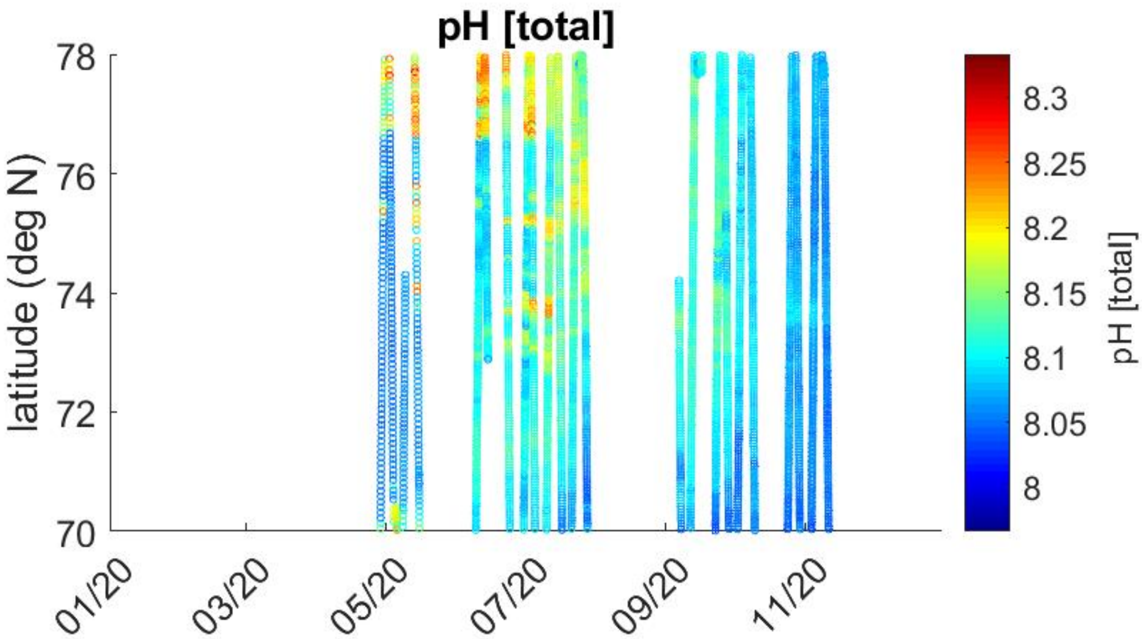


***Figure 2.3.5.*** *pH (total scale) in the Barents Sea Opening observed in 2020 by the spectrophotometric pH part of the combined pH/$CO_3$ sensor system. Tromsø, Norway is located at approximately 70°N and Longyearbyen, Svalbard is located at ~78°N. In May-June, pH was higher close to Svalbard (~77-78°N) and pH began to increase in the open ocean part of the transect (~72-76 °N) in July-September – the rise in pH was likely due to phytoplankton production and $CO_2$ drawdown. By October-November 2020, low-light wintertime conditions limit phytoplankton production and pH declines likely due to mixing up of deeper waters with lower pH and equilibration with atmospheric $CO_2$.*

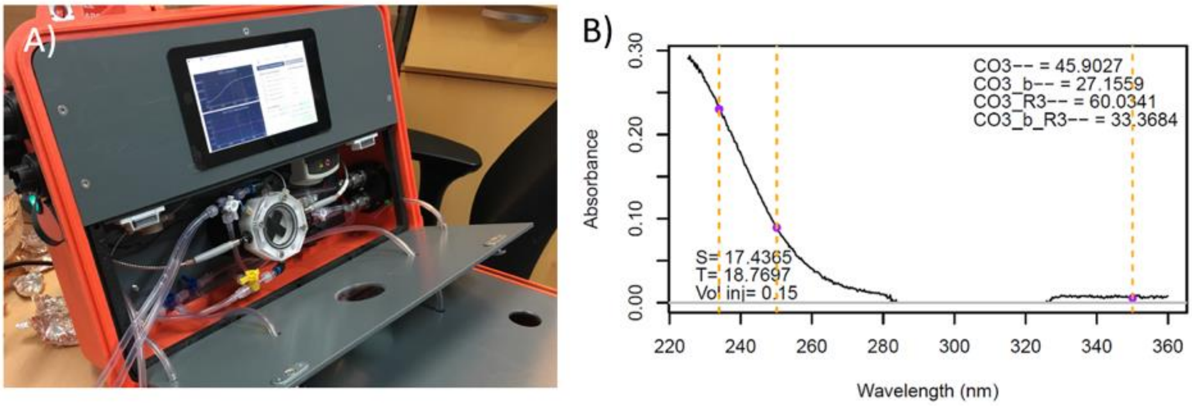


***Figure 2.3.6.*** *A) Photo of the $CO_3$ ion spectrophotometric sensor system that is designed to operate on a FerryBox in combination with a spectrophotometric pH sensor system. It is also designed to fit in a Pelicase (model 1500) for easy transportation and modular installation. This flow through sensor system is similar in design and function as the pH sensor system. B) Example of spectral data and calculation of $CO_3$ ion concentration based on absorbance at 234 nm and 250 nm with a control absorbance measurement at 350 nm based on a salinity-dependent algorithm (Sharp and Byrne, 2019).*

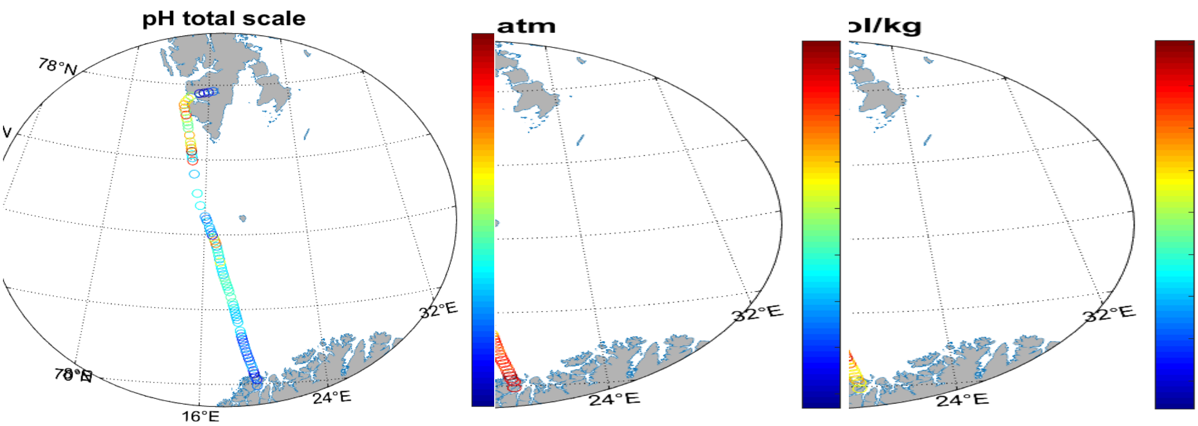


***Figure 2.3.7.*** *Preliminary combined observation data of pH (total scale), $fCO_2$ (µatm), and $CO_3$ ion (µmol $kg^{-1}$) (panels from left-right) on a Tromsø-Longyearbyen transect from 13-18 August 2021. The water mass near Tromsø and in the Barents Sea Opening was relatively low in pH and high in $fCO_2$, while the Arctic water mass close to Svalbard was higher in pH and lower in $fCO_2$ (with the exception of the water mass in Isfjorden), which is typical for summertime conditions. $CO_3$ ion concentrations were relatively high close to Tromsø and in the Barents Sea Opening and decreased to <~140 µmol $kg^{-1}$ close to Svalbard. The positive correlation between pH and $CO_3$ ion in the water mass near Svalbard is consistent with relationships in carbonate system chemistry.*

For the third activity, an integrated sphere absorption meter sensor (TriOS Measurement and Data Technology GmbH; OSCAR PSICAM) for measuring spectral absorbance (360-750 nm) was adapted to the Barents Sea FerryBox system. The PSICAM is designed for discrete sample and standalone operation, so this activity consisted of further developing it for flow-through operations using a series of Python-based software/GUI-controlled valves and pumps to fill and rinse the sensor with seawater, a cleaning bleach solution, milli-Q water, and an absorption standard (nigrosin) (Fig. 2.3.8), and also for communication between the FerryBox system and the PSICAM to allow for provision of sea temperature and salinity. Prior to deployment on the Barents Sea Opening FerryBox, series of tests were performed at the NIVA Research Station in Oslofjord in 2019-2020 using different batches of natural seawater, algal cultures, and artificial DOM additions (Fig. 2.3.9). The system was installed on the Barents Sea Opening FerryBox in 2021, but a failure in one of the source LEDs required the instrument to be sent back to the manufacturer for repair. The instrument has returned from the manufacturer and ready for re-installation and operation in August 2021. Like the pH/$CO_3$ system, the deployment of the PSICAM was delayed due to COVID-19 for the same reasons listed above.

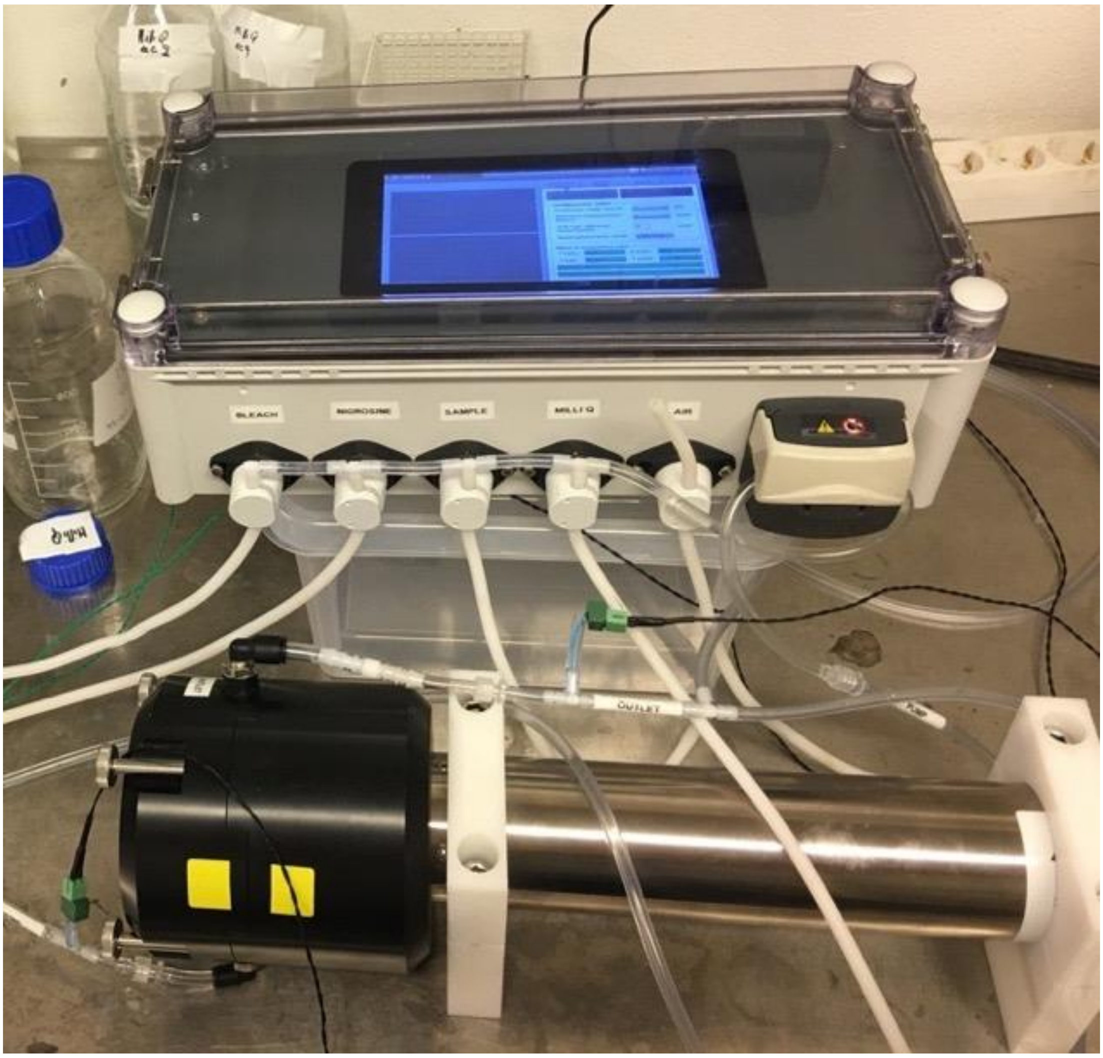


***Figure 2.3.8.*** *A photo of the PSICAM system in the lab before deployment. The system is designed to operate in unattended flow-through operation on a FerryBox. The PSICAM is in the lower part of the photo (black and silver with two white brackets) and the Raspbery pi/Python-based GUI/valve/pump control system is in the upper part of the photo with five electronically-actuated valves that control flow and drainage from the PSICAM and also allows for control and visualization of data via the touchscreen. A mini-peristaltic pump is also integrated into the control system to assist with rinse and calibration fluid movement.*

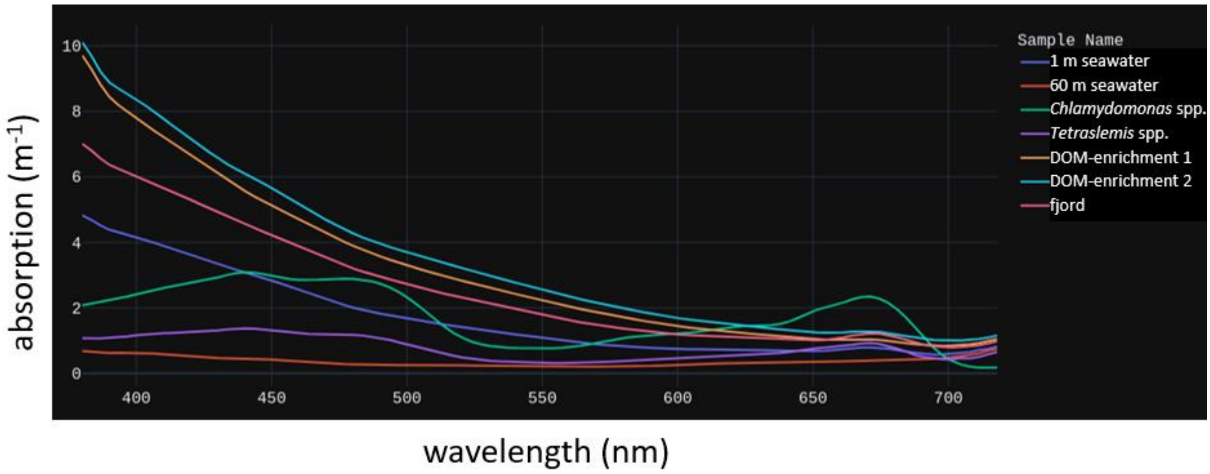


***Figure 2.3.9.*** *Spectral absorption measured by the PSICAM during tests at the NIVA Research Station using a variety of different natural seawater, algal cultures, and DOM-enriched sources. The two algal cultures show typical stronger absorbance around ~450-500 nm and ~650-700 nm due to chlorophyll and accessory pigments. The DOM-enriched samples (lignin) had strong absorbance in the blue part of the spectrum (<~500 nm) where DOM usually absorbs the most strongly at. The 60 m seawater had the lowest absorption indicating that it was low in DOM and particles.*

### 2.3.2. Lessons learned and technology challenges identified during the project

While this activity in Task 3.4 utilized existing technology, the assembly of the existing technology into a sampling or sensor system required a high level of hardware and software development at NIVA. This was the case for all three activities – the microplastics sampling system required development for control of pumping and measuring flow of large volumes of water; the pH/$CO_3$ sensor system used off-the-shelf light sources and spectrophotometers but otherwise required hardware fabrication and software design; and the PSICAM sensor system also required design and fabrication of the flow control system to allow for autonomous operations that an ocean observing system requires. The $CO_3$ portion of the pH/$CO_3$ sensor system posed a challenge in terms of converting existing knowledge about measuring $CO_3$ ion concentration in a benchtop spectrophotometer to a miniaturized and autonomous flow-through system. This included the testing and identification of a fit-for-purpose UV spectrophotometer as described above in addition to sourcing and designing the flow-through cuvette to use UV-transparent optical windows. Nonetheless, the advances made during the project were significant and brought open ocean observing systems closer to being fully operation in terms of autonomous/unmanned collection of microplastics particles from seawater, assessment of ocean acidification by measuring two carbonate system variables with relatively low volumes of seawater (100’s of ml per sample as opposed to 2+ L/min as required by $pCO_2$ sensors), and measurement of optical properties of seawater including chlorophyll, cDOM, and phytoplankton accessory pigments with a PSICAM.

### 2.3.3. Description of processing and analysis of the obtained data

The sensors and samplers implemented by NIVA in Task 3.4 include a microplastics sampler, a combined pH/$CO_3$ sensor, and an integrated sphere absorption meter sensor. Data that has been and will be collected from the sampler/sensors include time, latitude, longitude, temperature, salinity, chlorophyll a fluorescence at a fixed depth of ~5 m, in addition to the sampler/sensor specific data: microplastics concentration by size fraction; seawater pH (total scale) and $CO_3$ ion concentration (µmol $kg^{-1}$) accompanied by analysis temperature; and absorption spectra ($m^{-1}$) from 360-750 nm and analysis temperature for the PSICAM. Data are processed using Matlab/Python and assessed for quality based on established quality control routines for the sampler/sensor type and other similar underway data as well as for oceanographic consistency. The pH and $CO_3$ data will also be assessed using carbonate system algorithm software CO2SYS and Seacarb for agreement with discretely collected carbonate chemistry samples and $pCO_2$ sensor data.

#### 2.3.4. Accessibility of the obtained data sets and repositories used

All data will be stored on NIVA data servers. The FerryBox variables and metadata will be sent to the European FerryBox Database and EMODnet Physics repositories. All links will be provided to the INTAROS Data Catalogue.

#### 2.3.5. Future plans for operation of the observing system, including data provision

All three sampler/sensor systems are planned for continued operation on the Barents Sea Opening FerryBox system for the remainder of 2021 and into 2022. Continued development and testing of the $CO_3$ ion portion of the pH/$CO_3$ sensor and the PSICAM will continue, but at-sea development and testing is postponed until the shipping company allows scientists to travel with the ship again – this is expected to occur when COVID-19 vaccinations have been fully implemented and pre-pandemic operations resume.

*Data exploitation.* Data collected under Task 3.4 will be made available to the scientific community for synthesis and modeling work. The carbonate system data, after quality control and assurance, will be provided to ocean acidification data repositories related to UN Sustainable Development Goal (SDG) 14.3.1 Indicator calls for the "Average marine acidity (pH) measured at agreed suite of representative sampling stations".

### 2.4. CNRS-LOCEAN – endurance glider lines in Fram Strait

Contributors: Marie-Noelle Houssais, Christophe Herbaut, Laurent Mortier, Pierre Testor

#### 2.4.1. Results of the final implementation of the observing system

CNRS-LOCEAN has contributed to INTAROS through monitoring of the Atlantic Water Current properties at the entrance of the Arctic Ocean in Fram Strait and off North Svalbard. As part of this monitoring activity, regular gliders missions have been carried out in eastern Fram Strait since the beginning of the project during four successive summers (2017 to 2019). The duration of each mission was planned for approximately two months and the gliders would repeat every year, as far as possible, approximately similar sections across the West Spitsbergen Current (endurance glider lines).

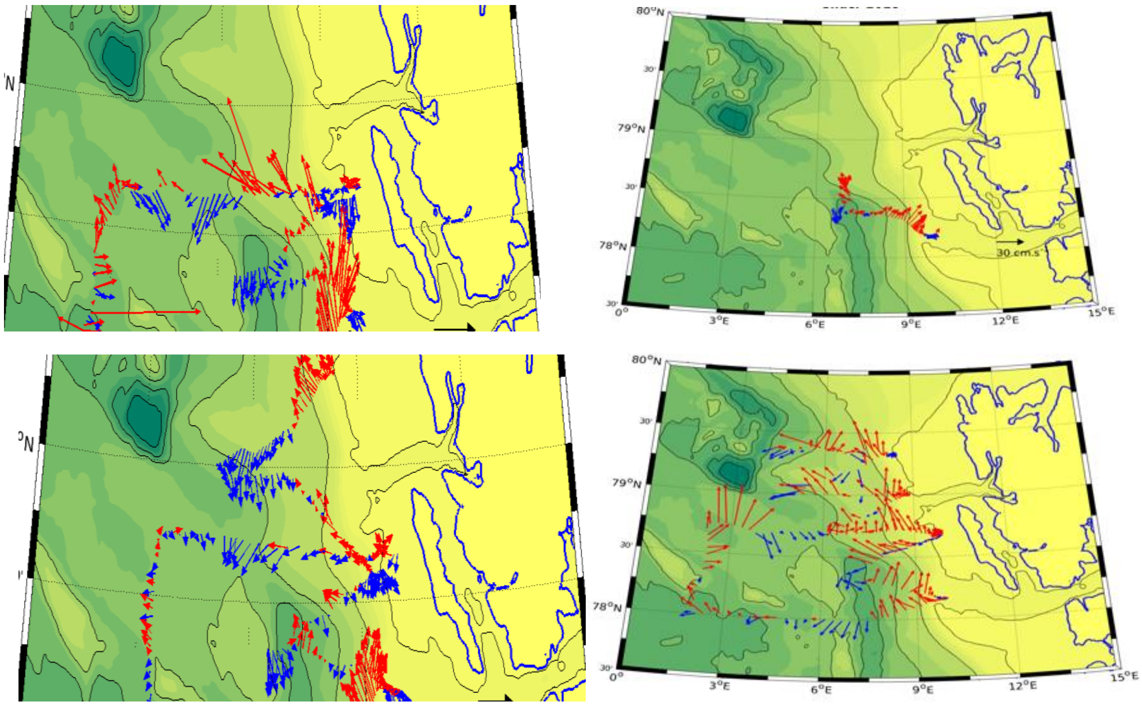

*Figure 2.4.1. The four glider missions carried out successively in summer 2017, 2018, 2019 and 2020. Also shown are the depth-averaged ocean velocities in the upper 1000 m as deduced from the glider trajectories. Arrows are colored in red (blue) if velocities have a northward (southward) meridional component.*

In 2018 and 2019, we were able to plan simultaneous deployment of two gliders. Unfortunately, in 2018, one of the gliders suffered from damage during its transportation to port and, in 2019, technical issues with glider "Campe" led to cancelation of the mission before the end of the mission for urgent recovery. Technical issues also obliged us to shorten the Tintin mission in July 2018.

All gliders were equipped with classical sensor payload allowing to monitor physical (conductivity, temperature, pressure, dissolved oxygen) and optical (Chla fluorescence, CDOM fluorescence, turbidity or backscattering) properties of the water column (Table 2.4.1).

*Table 2.4.1. Glider missions carried out in Fram Strait during INTAROS*

| Year | Glider type/ID | Deployment date | Recovery date | Deployment position/vessel | Recovery position/vessel | Sensor payload |
|---|---|---|---|---|---|---|
| **2017** | Slocum G1 SN127 Tintin | 25/07/2017 | 22/09/2017 | 78°40'N-09°15'E RV Oceania | 78°12'N-07°18'E RV Pourquoi Pas ? | CTD-SBE41CP (pumped), Wetlabs FLBBCD, Aanderaa Optode 3835 |
| **2018** | Slocum G1 SN127 Tintin | 06/07/2018 | 14/07/2018 | 78°11'N-10°E RV Oceania | 78°35'N-07°E NRV Alliance | CTD-SBE41CP (pumped), Wetlabs FLBBCD, Aanderaa Optode 3835 |

| | | | | | | |
|---|---|---|---|---|---|---|
| **2018** | Slocum G1 SN070 Potame | Not deployed | -- | -- | -- | -- |
| **2019** | Slocum G1 SN176 Campe | 13/07/2019 | 24/07/2019 | 78°49.4'N-09°27'E RV Oceania | 79°08'N-07°10'E Anakena | CTD-SBE41CP (pumped), Wetlabs FLBBCD, Aanderaa Optode 4831F |
| **2019** | Slocum G2 SN246 Thèque | 13/07/2019 | 08/09/2019 | 78°49.4'N-09°25'E RV Oceania | 78°40'N-09°54'E KV Svalbard | CTD-SBE41CP (pumped), Wetlabs FLNTU, no optode |
| **2020** | Seaglider SN149 Phéidippides | 25/07/2020 | 25/09/2020 | 78°10'N-10°E RV Oceania | 79°01'N-11°37'E Jean Floc'h | CTD-SBE41 (unpumped), Wetlabs BB2FL-VMT, SBE43F |

Transects at different latitudes allowed us to describe the West Spitsbergen Current structure along the varying bottom topography toward the Arctic. Regular snapshots of the same transect highlighted the variability of the current, as exemplified in Figure 2.4.2 by the substantial salinity decrease in the AW layer after 2017.

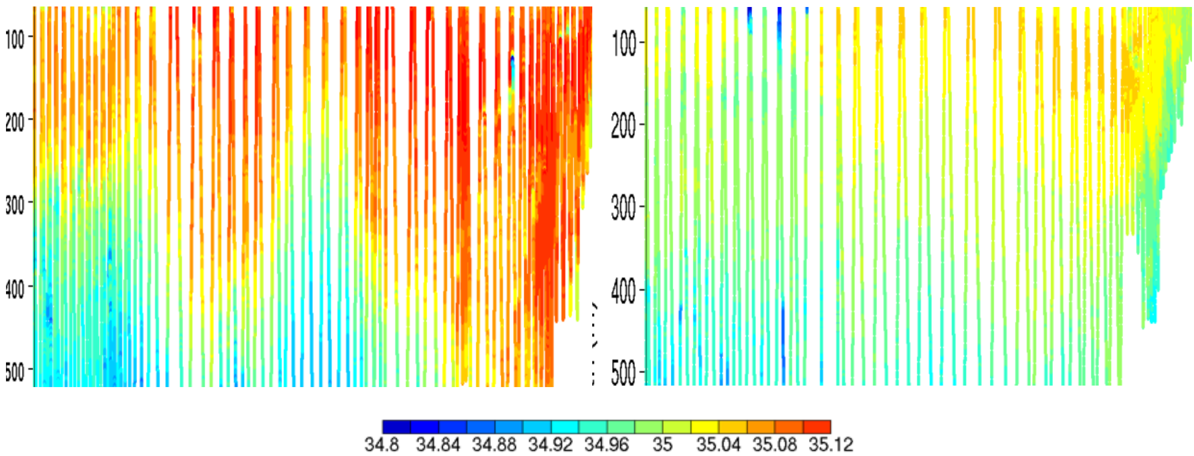


***Figure 2.4.2.*** *Salinity distribution along a transect at 78°40'N carried out between (left) 27 July- 4 August 2017 and (right) 17-23 July 2019*

### 2.4.2. Lessons learned and technology challenges identified during the project

Several challenges have been identified in relation to glider deployment in Fram Strait:

- Navigation in ice-covered water is not feasible if gliders are not able to surface for GPS positioning and communication to land via satellite. In particular the lack of communication hampers near real time control by the pilot on glider trajectory. In order to avoid such situations, it was decided to limit our glider missions to the open water part of the strait which puts strong constraints on both the geographical coverage of the mission (mostly confined to the southeastern part of the strait) and the time of operation (late summer-early fall being the most favorable season). Real time adjustment of the glider mission to ice conditions based on the best available sea ice products was therefore needed. In addition, to avoid undesirable glider surfacing under possibly undetected ice floes, an ice detection software based on the ISA algorithm (Klatt et al., 2007) was tested. However, the software revealed to impact the ice navigation and needs to be better evaluated before being used routinely.

- Control of glider trajectory revealed to be challenging in a boundary current type of environment with high velocity (several tens of cm/s) like the West Spitsbergen Current. In particular it was challenging to maintain the glider heading along a transect that would map the density distribution perpendicular to the (mostly along-slope) current direction in order to retrieve the main geostrophic component of the flow. Constant adjustment of the way points during glider mission however led to rather successful mapping (Fig. 2.4.1).

- Time-space constraints on the glider mission as explained above and considering also the limited battery autonomy of the Slocum, made it difficult to schedule the exact dates of the mission. While deployment could always be made at the desired location on the West Spitsbergen shelf thanks to the support of our colleagues from IOPAN (Poland) on board RV Oceania, recovery was always subject to the availability of a vessel at the right time and location on site. This could be sometime challenging in an environment where the glider is not easily maneuverable due to high current velocities and the location of the sea ice edge is changing rapidly. In 2020, we were able to recover the glider from ashore using the coastal boat operated by the French Polar Institute from Ny-Alesund, a solution that may be used more systematically in the future if the glider can be guided to the entrance of Kongsfjorden.

### 2.4.3. Description of processing and analysis of the obtained data

Based on endurance glider lines at different latitudes across the West Spitsbergen Current, we were able to collect a comprehensive dataset that describes the physical (and partly biogeochemical) environment of eastern Fram Strait across a domain extending (depending on year) from ca. 78°N to 79°40’N and from the West Spitsbergen shelf to 2°E longitude.

Delayed mode data are further processed, using a software that generate profiles based on time series data. These data are then quality checked for thermal lag bias (Garrau et al., 2010), spurious profiles or proper dark count adjustment of optical probes. However, this later step has still to be standardized using commonly agreed best practices (an OceanGliders Best Practices workshop, under the OceanGliders GOOS Associated Programme, https://eurosea.eu/download/news_and_events/OceanGliders-Best-Practices-Workshop-May-2021.pdf, was recently organized by H2020 EuroSea to review and harmonize the data processing).

### 2.4.4. Accessibility of the obtained data sets and repositories used

Real time data are stored in the Coriolis database (www.coriolis.eu.org). A Doi has been attributed to the data via Seanoe (eg https://doi.org/10.17882/51473 for the 2017 data) where data are made available upon request. Data can also be visualized from the EGO glider deployment catalogue using a dedicated website interface (for the Fram Strait Observatory see: https://www.ego-network.org/dokuwiki/doku.php?id=public:operationsintheatlantic#Fram%20Strait%20Observatory ).

### 2.4.5. Future plans for operation of the observing system, including data provision

Within the INTAROS project, a set of so-called "endurance glider lines" have been maintained west of Svalbard to monitor the physical properties of the West Spitsbergen Current and the transports associated with the Atlantic inflow to the Arctic Ocean. This inflow is of major importance for the dynamics of the interior Arctic Ocean and Fram Strait constitutes its major choke point where sustained monitoring is highly relevant. Our repeat transects revealed interesting geographical contrasts (both in the off-shore and along-shore directions) and temporal variability (both at the intra-seasonal time scale and between years) in the flow properties in the strait at high spatial (down to a few km) and temporal (down to a week or so) resolution. While the mooring array which has been maintained across Fram Strait since the mid-90s (e.g. Beszczynska-Möller et al, 2012) and regular oceanographic cruises (e.g. Walczowski et al., 2017) are providing valuable estimates of the flow and transports, glider transects add highly valuable, complementary information regarding the fine scales which are known to play an important role in the flow dynamics, especially recirculations and eddies which are known to control the net transports to the Arctic Ocean. In this respect glider endurance lines should be continued in this region. Yet, optimization of their exact location, time of implementation and repeatability is a key element of such a long-term monitoring programme. The information gained from glider missions during INTAROS combined with the wider context provided by model simulations and other conventional observations should be a key element in this process.

*Data exploitation.* Glider data from endurance glider lines can be used for assimilation in global or regional ocean reanalyses (Mercator), forecast systems and marine services. They will also be combined with other ocean data products in the context of multi-purpose/multi-disciplinary observatories (like Fram Strait Hausgarten, Arctic ROOS, SIOS, ...), providing complementary information on ocean fine scales.

## 2.5. CNRS-Takuvik – BGC Argo floats in Baffin Bay

Contributors: Marcel Babin, Claudie Marec, Marie-Hélène Forget, Achim Randelhoff

### 2.5.1. Results of the final implementation of the observing system

**Field work**

The contribution of CNRS-TAKUVIK to INTAROS WP3 “Enhancement of multidisciplinary in situ observing systems” is made through the monitoring of the biogeochemical properties of the Baffin Bay with the deployment of a fleet of BGC Argo floats dedicated to navigating in ice-infested waters.

To study the onset of a Phytoplankton Spring Bloom event under melting sea ice in May to its conclusion within the SIZ in July, as well as late fall and winter ecosystem properties, Takuvik has deployed a fleet of BGC Argo floats (called ProIce, dedicated to polar environments) in Baffin Bay since the beginning of the program.

Each BGC Argo float is equipped with the following payload until fall 2020:

- CTD (Conductivity, temperature, depth)
- Radiometer: OCR wavelengths: 380, 412, 490nM, PAR,
- fluorescence chl-a,
- fluorescence CDOM,
- Backscattering,
- Suna (nitrates),
- Optode (Dissolved Oxygen)

The deployments were staggered in time as indicated in Table 2.5.1.

*Table 2.5.1 Timeline of BGC Argo floats deployed in Baffin Bay in 2016-2021*

| 2016 | 2017 | 2018 | 2019 | 2020 | 2021 |
|---|---|---|---|---|---|
| 5 floats | 7 floats | 2 floats<br>+ 2 recovered (1 destroyed) | 3 floats<br>+ 2 recovered | Depl. cancelled (COVID)<br>+ 1 recovered | 4 refurbished and upgraded floats to be deployed in October |

Deployments scheduled in Summer 2020 were cancelled due to COVID situation. Besides, over the program, 5 floats were recovered: 1 destroyed, 4 were refurbished.

We intend to launch 4 floats in October 2021 (cruise dedicated to the fall-winter transition of the Arctic ecosystem), which are refurbished and upgraded BGC Argo floats. They present a more flexible firmware. Therefore, they will support a more sophisticated payload.

A brand new and highly sensitive radiometer (MPE radiometer, by Biospherical Scientific Instruments) designed upon request of Takuvik will be implemented on these platforms for the next deployments, in addition to the initial payload.

One of these floats will also be equipped with a new sensor dedicated to measure particle size abundance (UVP6 by Hydroptics). This will give a complementary information to characterize the ecosystem. The implementation of this sensor will be a “premiere” on an ARGO float in Arctic.

### 2.5.2. Lessons learned and technology challenges identified during the project

An ice-covered ocean presents a real challenge for Argo floats that must surface for geo-localization and to use satellite networks for data transmission and command reception. Therefore, technical adjustments are required to make the floats as much as possible operational in the Arctic Ocean, in particular with essential ice-detection systems to prevent them from surfacing in ice-covered waters (see details in Andre et al., 2020). ISA (ice sensing algorithm, Klatt et al., 2007) had to be adapted to the regional conditions and corrected as it went along.

Although the ProIce floats were adapted to ice-infested water navigation, the operation in this context remains a real challenge.

Almost 2000 profiles have been acquired so far with unprecedented sets of data with series measured under ice during wintertime (2 winters under ice for takapm016b, 1 winter under ice for takapm011b, takapm012b, takapm017b, takapm018b, takapm020b).

*Table 2.5.2. Summary of deployed BGC Argo floats and their characteristics (2016-2020)*

| | WMO | First profile | Last profile | Nb of profiles | ISA threshold | Comment |
|---|---|---|---|---|---|---|
| **takapm014b** | **6902668** | 09/07/2016 | 31/10/2016 | 99 | -1.1°C | Disappeared during 1st winter |
| **takapm005b** | **4901803** | 09/07/2016 | 31/10/2016 | 98 | -1.1°C | Disappeared during 1st winter |
| **takapm009b** | **6902667** | 09/07/2016 | 31/10/2016 | 99 | -1.1°C | Disappeared during 1st winter |
| **takapm013b** | **4901802** | 09/07/2016 | 31/10/2016 | 98 | -1.1°C | Disappeared during 1st winter |
| **takapm019b** | **4901801** | 30/05/2016 | 25/05/2017 | 363 | -1.1°C | (no BGC payload only O2) |
| **takapm008b** | **6902669** | 20/07/2017 | 03/11/2017 | 102 | -1.1°C | Disappeared during 1st winter |
| **takapm012b** | **4901805** | 20/07/2017 | 12/08/2018 | 124 | -1.3°C | Recovered – refit |
| **takapm006c** | **4901804** | 20/07/2017 | 29/07/2017 | 12 | -1.3°C | Lost after grounding |
| **takapm015b** | **6902670** | 20/07/2017 | 05/11/2017 | 113 | -1.3°C | Surface-blocked on Last descent |
| **takapm017b** | **6902829** | 23/07/2017 | 9/04/2018 | 106 | -1.3°C | Destroyed upon recovery |
| **takapm007b** | **6902666** | 23/07/2017 | 27/09/2017 | 70 | -1.3°C | Lost after grounding |
| **takapm016b** | **6902671**<br>**6902953** | 23/07/2017 | 29/7/2019 | 185 | -1.3°C | Remote firmware upgrade (change of WMO) |
| **takapm020b** | **6902897** | 17/7/2018 | 12/10/2019 | 186 | -1.3°C | Recovered for refit |
| **takapm011b** | **6902896** | 17/07/2018 | 31/05/2019 | 133 | -1.3°C | Flooded after Ice contact |

| | | | | | | |
|---|---|---|---|---|---|---|
| **takapm018b** | **6902967** | 14/07/2019 | 20/10/2020 | 196 | -1.3°C | Recovered for maintenance and refit |
| **takapm004b** | **4901806** | 17/07/2019 | 02/09/2019 | 8 | -1.3°C | Recovered for maintenance and refit |

Among the lessons learnt, we identified one main reason of float losses at the beginning of the study. We also acquired a better control in programming for a safer navigation in icy conditions (the study focuses on Baffin Bay, which involves navigational challenges for floats in terms of bathymetry, ice coverage and circulation). We also managed to recover up to 5 floats before their batteries collapsed.

As it went along, we also underlined that the float was missing flexibility in terms of sensors integration. This led us to perform upgrades of the platforms that we will deploy in 2021.

Besides, we realized that the commonly used radiometry sensor (OCR4) is not able to measure very low light levels under ice, conditions encountered by the floats in late winter and early spring. Takuvik worked with Biospherical Scientific Instruments on the design of a highly sensitive radiometer (MPE) that will be added to the initial payload for fall 2021 deployments. This should enable to quantify very low levels of light under ice that it is impossible to do with current float sensors. This is essential to compute the specific phytoplankton growth rates and to improve the under-ice light models.

The UVP6 (Hydoptics), a sensor dedicated to measure particle size abundance will also give complementary information to characterize the ecosystem. One of the four floats to be deployed in 2021 will be equipped with such sensor.

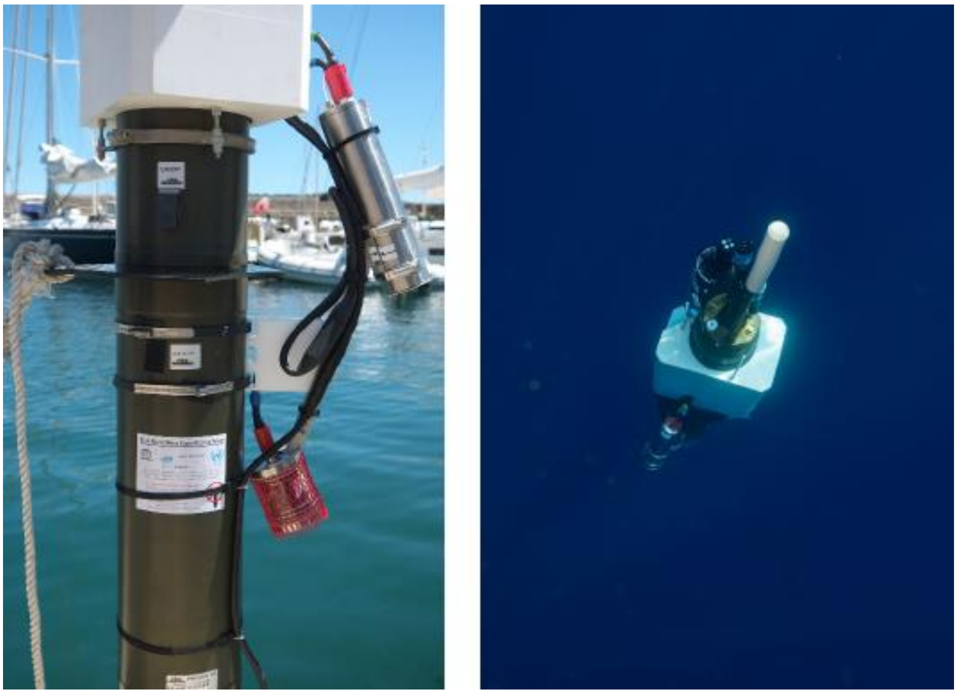

***Figure 2.5.1.*** *ProIce float equipped with an UVP6, credit LOV.*

#### 2.5.3. Description of processing and analysis of the obtained data

We collected an original dataset from the Arctic Ocean (Baffin Bay) with a fleet of BGC-Argo floats, including bio-optical and biogeochemical properties of the marine ecosystem. Data acquired by Takuvik's ProIce floats are available in real time and free of access in the Argo database on the Coriolis (GDAC) online platform.

Delayed mode qualification for Pressure, Temperature and Salinity was processed by Coriolis. The quality control of biogeochemical parameters was performed according to X. Xing procedure as described in the supplemental material of Le Traon et al. (2020).

https://www.frontiersin.org/articles/10.3389/fmars.2020.577408/full#supplementary-material

Delayed mode BGC data is currently being compiled in the Coriolis database.

#### 2.5.4. Accessibility of the obtained data sets and repositories used

Data is available in free access via the ftp dataset on the Coriolis website. http://www.coriolis.eu.org/Data-Products/Data-Delivery

The data are also available on a new European web portal to access Argo data: https://dataselection.euro-argo.eu/

This powerful web interface allows selecting, visualising and downloading Argo profile data. In addition to the usual NetCDF format, the tool offers the possibility to download Argo profiles in .csv format. It replaces https://fleetmonitoring.euro-argo.eu/dashboard

Data is also available on the LEFE Cyber Database

http://www.obs-vlfr.fr/proof/php/GREENEDGE/greenedge_autonomous.php

WMO numbers of the platforms are given in the table above.

#### 2.5.5. Future plans for operation of the observing system, including data provision

The BGC Argo floats will continue to gather data as long as the platform are operational. Recovery, refurbishing and re-deployment will take place when possible.

The new sensors integrated on the platforms will enhance the environmental dataset to characterize the ecosystem and will be added to the Coriolis platform as well as the LEFE Cyber Database.

The lack of geo-localization of under-ice profiles remains an issue that should be thoroughly addressed in near future.

### 2.6. NERSC and contribution from the collaborating project CAATEX

Contributors: Hanne Sagen and the CAATEX consortium.

As part of the CAATEX program NERSC coordinated and implemented three field experiments and two cruises as part of the UAK project. Through these projects NERSC provided ship time and technical support to the INTAROS Task 3.2 (North of Svalbard) and Task 3.5 (Central Arctic). The CAATEX project and cruises are described below, while the UAK project are described in D7.11. CAATEX is funded by the Research Council of Norway and Office of Naval Research. The UAK project is funded by the Research Council of Norway through the INTPART program.

CAATEX is a joint U.S.-Norwegian acoustic thermometry experiment across the Arctic basin. The CAATEX experiment was designed to be comparable to a previous trans-Arctic propagation experiment, the 1994 Trans Arctic Propagation (TAP) experiment. The purpose was to capture the change in acoustic propagation of low-frequency sound across the Arctic basin due to changes in ocean stratification, mean ocean temperature and sea ice conditions. The goal is to explore the fundamental limits to exploit the acoustic remote sensing capabilities to characterize the large-scale properties of the Arctic Ocean.

Two acoustic sources transmitted low-frequency (35 Hz) sound, one source transmitted from Nansen Basin in the Eastern Arctic, and a second source transmitted from the Beaufort Sea in the Western Arctic. The source moorings and four other receiving moorings were equipped with 25-40 hydrophone vertical arrays. The moorings were deployed along the path crossing the Arctic Ocean. The moorings successfully recorded transmissions every 36 hours during a yearlong deployment from fall 2019 to fall 2020. All six moorings were equipped with oceanographic instruments for salinity and temperature measurements, an upward-looking sonar to measure the ice thickness, and pressure gauges to measure the ocean bottom pressure.

The comparisons of acoustic measurements from 1994 will contrast present-day heat content to the past measurements, but also to other environmental changes. The acoustic arrival structure can reveal changes in the vertical stratification. Transmission loss measurements may provide information about changes in the ratio of first-year ice to older ice. Acoustic scattering, which diagnoses the strength of internal-wave activity that can change the vertical stratification. Finally, the acoustic signal propagation and ambient noise obtained by this experiment will improve our ability to monitor, communicate and navigate in the Arctic Ocean.

In the following we provide some information about the CAATEX cruises which provided support to INTAROS activities.

### 2.6.1. CAATEX 2019

The Coordinated Arctic Acoustic Thermometry Experiment (CAATEX 2019) research cruise was conducted with the Coast Guard vessel KV Svalbard in the Arctic Ocean from August 14 to September 9. The CAATEX 2020 cruise was coordinated by Nansen Center, and eight other Norwegian and international research institutions participated in the cruise. The main goal of the cruise was to deploy three acoustic rigs, four buoys to drift with the ice, and one oceanographic rig for the INTAROS.

The CAATEX acoustic network consisted of 6 acoustic moorings – three moorings in the eastern Arctic and three moorings in the western Arctic. The acoustic rigs were designed collect ocean point measurements at different depths data and acoustic reception data. To make the data processing uniform the moorings were built using the same design and instrumentation. Each CAATEX moorings were around 4000 m long, and they stand vertically in the water column by means of heavy anchor and buoyancy spheres at the top. The rigs were equipped with oceanographic instruments for point measurements of salt and temperature, ocean currents, ice parameters and the pressure on the bottom. The deep-water moorings were designed to be recovered in dense and drifting sea ice building on experiences made by the CAATEX partners (NERSC, SIO and WHOI) in the Fram Strait and in the Beaufort Sea.

The Norwegian CAATEX project was responsible for deployment of three moorings in the Nansen Basin. The deployment cruise was carried out with support from the Norwegian Coast Guard using the icebreaker KV Svalbard. The actual deployment array of acoustic moorings deviated significantly from the planned array primarily due to a Russian short notice missile exercise at the North Pole, but also because of rough ice conditions in the North pole region. See Fig. 2.6.1 for the planned and the actual deployment.

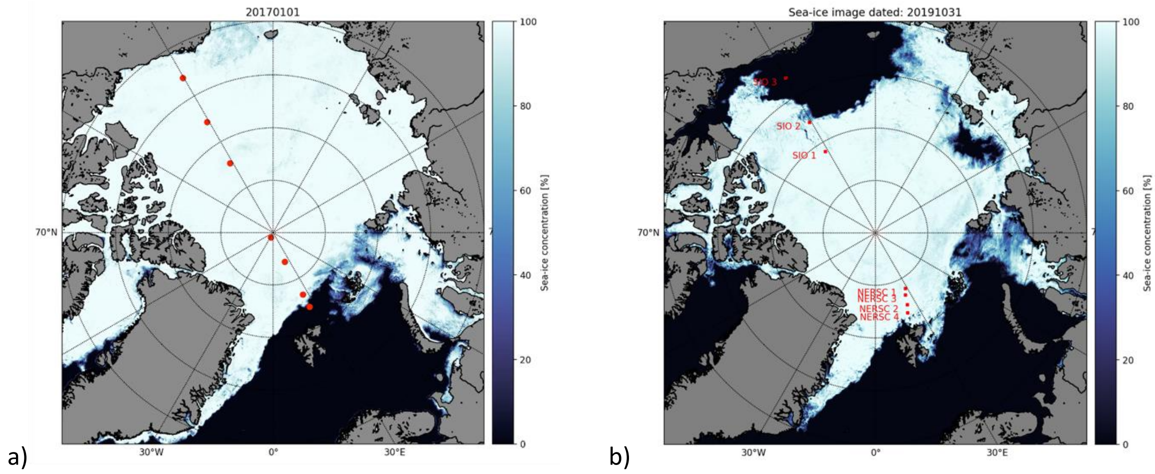


***Figure 2.6.1.*** *Planned and actual deployment of the CAATEX mooring array.*

The deployment of rigs was challenging due to varying ice drift conditions and that the bottom topography in large parts of the Arctic Ocean is not adequately mapped and known. Therefore, before deploying each rig, the bottom topography must be measured and mapped in an area with a radius of more than 30 kilometers around the selected position. This mapping was challenging in tight pack ice. Furthermore, variation in ice drift must be carefully monitored before and during the 7-9 hours it takes to put the rig to a depth of 4000 meters. All four rigs (including NERSC-4 mooring) were successfully deployed with the careful planning, previous experience, good information about the weather and ice conditions on site and a skilled crew. As part of the CAATEX program an Ice tethered profiler was deployed at the North Pole for the WHOI and an acoustic receiver buoy was deployed to listen to the acoustic transmissions. The CAATEX project provided two mooring technicians and rental of a mooring winch appropriate for deployments in ice. This facilitated the mooring deployments and recoveries for CAATEX, but also for the INTAROS moorings.

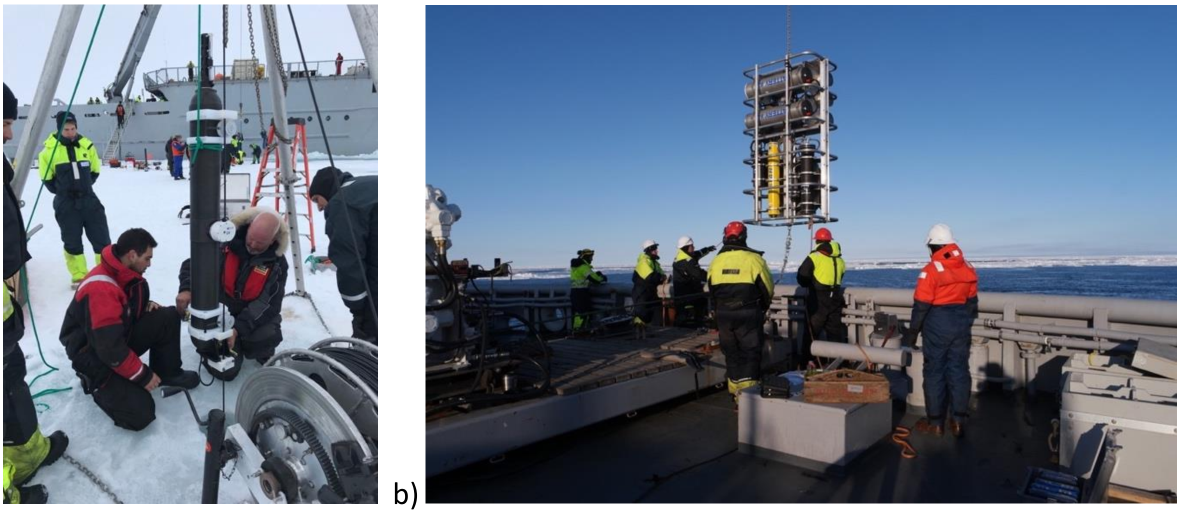

a) b)

*Figure 2.6.2. (a) Deployment of the ITP at the North Pole 21 August 2019 and (b) deployment of the acoustic source.*

A multidisciplinary mooring was deployed for the INTAROS project (IOPAN, UIB, NERSC). Two SIMBA buoys were deployed for the INTAROS project (FMI) which gathered information about the ice and how it would grow and vary in thickness throughout the winter and again how it would melt during the coming summer season. All buoys drifted with the ice from the North Pole towards the Fram Strait, while continuously collecting environmental information about the sea under the ice, about the nature of the sea ice and about the air near the ice. The data from these buoys can provide information on where and in what part of the year the ice melts most from the underside that is in contact with a warmer seawater or where and when it melts from the surface in contact with warmer air layers.

A total of nine ice stations were conducted. At the ice stations, ice cores were drilled and taken to study the structure of ice in laboratories. Measurements of ocean currents and turbulence under the ice, measurements of light and algae, as well as passive measurements of sound were made. Larger areas around KV Svalbard were investigated using drones equipped with various remote sensing sensors to map sea ice and leads. Regular sea ice observations were conducted using the Arctic Shipborne Sea Ice Standardization Tool (ASSIST) developed by the International Arctic Research Center in Fairbanks.

### 2.6.2. CAATEX 2020-Nansen Basin

The Coordinated Arctic Acoustic Thermometry Experiment (CAATEX 2020) recovery cruise was carried out from 17 July to 10 August 2020 with the Norwegian Coast Guard vessel KV Svalbard in the Nansen Basin. The CAATEX 2020 cruise was coordinated by the Nansen Center. The activities during the cruise were:

1) Recovery of three moorings for the Coordinated Arctic Acoustic Thermometry Experiment – CAATEX project.
2) Recovery of four moorings for INTAROS (CNRS-LOCEAN, IOPAN, NERSC, UiB).
3) Rescue of one mooring for third party (CNRS-LOCEAN internal program).
4) Deployment of drifting ice buoys for the International Arctic Buoys Program - CAATEX.
5) Deploy 400 small wooden boats for outreach purposes (Float Your Boat).
6) Deployment of AIS buoys for monitoring of sea ice movement (CAATEX).
7) Sea ice in situ observation, radar and drones (INTAROS).

Some extra challenges in the planning of the cruise due to the CoVid19 situation. However, all tasks were successfully carried out.

#### 2.6.3. CAATEX 2020-Beaufort Sea

The Coordinated Arctic Acoustic Thermometry Experiment (CAATEX 2020) were carried out in the period from 12 October to 25 November 2020 with the Norwegian Coast Guard vessel KV Svalbard in the Arctic Ocean including the Beaufort Sea. CAATEX2020 cruise was coordinated by Nansen Center together with the Norwegian Coast Guard. The activities during the cruise were to recover four CAATEX moorings including one INTAROS mooring and to deploy 10 ice buoys for the international Arctic Buoy program.

This cruise was carried out as a mooring rescue operation using the KV Svalbard due to a breakout of a fire in the engine of the USCG Healy the 18 August 2020 just after departure for recovery of the acoustic moorings in the Beaufort Sea. The recovery cruise in Beaufort Sea (led by Scripps Institution of Oceanography) was cancelled, and the situation was critical if we could not recover the CAATEX moorings. This was because the atomic clocks in the tomographic instruments would empty the batteries, and thereby make it impossible to provide accurate timing of the travel time measurements due to clock drift. Nansen Center contacted the Norwegian Coast Guard who confirmed that they could carry out the operation. The approval went all the way up to minister level in Norway, and the final approval were given just a few days before departure 12 October. This operation was an example of good collaboration at different levels and across the Arctic Basin. All four moorings were recovered in darkness and under extreme temperatures. More details are found https://www.marinelink.com/news/value-friends-highlatitude-places-486531. The KV Svalbard travelled 7000 nautical miles in total distance of which 3500 nm with icebreaking.

a)  b) 

*Figure 2.6.3. The temperature were -40 degrees during the recovery of SIO-1 mooring and the photo (a) shows the acoustic source safely back on deck. (b) The top of the last mooring (SIO-3) which was trapped under the ice. It took two days with intense effort to recover this last mooring. The coast guard officer Andreas Soløy dived to locate and attach the mooring. All instruments were saved.*

### 2.6.4. Accessibility of the obtained data sets and repositories used

Data from 375 instruments distributed between 6 moorings have been collected as part of CAATEX. CAATEX data are currently being processed and analyzed within the CAATEX project with funding from Office of Naval Research and Research Council of Norway. These data are not part of the INTAROS data portfolio and will follow its own data management plan. Thus, the CAATEX data and analysis results will be published along with data products through the Norwegian Marine Data Center. This is in line with data policies at NERSC, and data formats will build on standards developed for ocean moorings in INTAROS.

# 3. Performance and fitness-to-purpose of the platforms, sensors and systems implemented during INTAROS for a future sustained Arctic observing system

## 3.1. IOPAN

**Drifting ice-tethered IAOOS platform in the central Arctic Ocean**

A short lifetime of the IAOOS ice-tethered platform deployed by IAOOS-Equipex for INTAROS resulted in a very low data return from an expensive asset. It was the main argument for reconsidering a choice of observing technology for providing ocean and sea ice data from a deep basin of the Arctic Ocean during the following field season. Additionally, the process of acquiring the platform from the IAOOS-Equipex consortium was highly demanding and time-consuming due to acquisition of a non-commercial product from a scientific group with no established procedure for an international purchase (prolonged contract negotiations, lack of proper documentation). The IAOOS-Equipex ice-tethered platform is a promising technology for atmosphere, ice, snow, and ocean observations in the Arctic that has already proved to provide valuable data published by the IAOOS-Equipex team (e.g., Koenig et al., 2016; Provost et al., 2017; Mariage et al., 2017; Athanase et al., 2019). However, based on INTAROS experience, at the current stage the platform has not yet reached the TRL (both in terms of platform maturity and availability) that allows for its wide operational application by external users (i.e., from outside the IAOOS-Equipex consortium).

**Deep ocean multidisciplinary mooring deployed in the Nansen Basin**

Oceanographic moorings deployed in fixed locations for longer periods are the only way to obtain year-round and high temporal resolution observations of subsurface physical, and biogeochemical variables in fixed location in the ice-covered regions of the Arctic Ocean.

Sensors and instruments implemented under INTAROS on the deep mooring in the Nansen Basin for measurements of physical variables as temperature, salinity, pressure, and ocean currents represented the well-proved and robust technologies that worked with no significant failure during year-long deployment in 2019-2020. Robustness is a key requirement for any long-term observing component of a sustained Arctic system, in particular for moored platforms which can be turned around only once a year (or more). While new technical solutions are indispensable for improving and extending the capabilities of an observing system, they should be extensively tested until reaching a high TRL before operational implementation as a component of the long-term observatory. To ensure the continuous temporal coverage and coherence of sustained observations, the core set of sensors and platforms should be available at least in duplicate to allow for necessary calibrations and repairs between long-term deployments (this seems to be an obvious requirement, but it is not always the case due to limited means). Additionally, development of the backup data storage system for instruments located at one mooring could be advantageous in the case of an instrument total failure (including data loss).

Endurance time of all moored self-recording instruments and sensors is mostly limited by battery capacity. For one-year-long deployments and using the optimized sampling rate, all implemented instruments were able to deliver the full data record while is the case of longer deployments (not intentional but due to ship unavailability or ice conditions hindering the mooring recovery) measurements usually stopped prematurely. There is a significant progress in power usage of newer sensors but in general battery lifetime in cold arctic waters is shorter than in other regions and instruments with higher energy consumption (e.g., active acoustic profilers) have limited endurance.

In a future sustained observing system, containing among other components the fixed moorings with multidisciplinary instrumentation, main problems include availability of more efficient power supplies and remote data retrieval. For some sensors (mostly biogeochemical), sensor stability and calibration also pose a challenge.

Moorings that are operated in the ice-covered areas in the Arctic Ocean should be equipped to the maximum extent with the location and recovery aids, including satellite beacons, acoustic transponders, avalanche beacons, and possibly also strobe lights. All devices that can help to locate and follow a mooring under and in ice significantly lower the recovery risk and increase safe data and instruments return.

Since an access to ship time on ice-capable vessels equipped for mooring operations in ice-covered waters is very limited and often based on collaborations with and using opportunities of other programs and project, moorings should be designed, build and prepared in such a way that any trained mooring technician (with no specific knowledge of a specific mooring) should be able to recover and deploy it even if the mooring owner/operator cannot participate in a cruise. This includes the full technical documentation, certificates and manuals for mooring hardware and instruments, necessary soft- and hardware, and extensive personal communication.

## 3.2. FMI

**SIMBA snow and ice mass balance buoys**

We suggest cryosphere society should use every possible Arctic field platform to deploy as many as possible SIMBA buoys. This is largely because SIMBA is an affordable device and deployment is relatively easy to do. It is recommended that INTAROS partners may consider their own SIMBA program, similar like FMI lake SIMBA program, so in case if there are field platform opportunities, the contribution can be made on time without delay. A good integrated monitoring system require sustainable maintenance and operation, so we need to have the ability to carry out field deployment successively since SIMBA has a lifetime of about a year. It would be nice that there are SIMBAs operated in the Arctic Ocean at any time.

Development of SIMBA algorithm is vitally important if SIMBA data is used for operational service.

A SIMBA consortium is recommended to be established along research institutions, universities, and other relevant organizations. The goal for SIMBA buoy would be an online post-processed data service provided to the stakeholders and the general public in real time. To provide high quality SIMBA operational data service, there is still a long way to go both technically and scientifically.

**Fixed station and UAV-based radiation measurements during the MOSAiC expedition**

In situ sea ice surface radiation budget is traditionally measured with fixed, surface-based stations powered with batteries, solar panels, or the ship generator. The two-source power supply system (a battery-based circuit associated to the power cables connected to the ship generator) developed for our FMI station proved successful in the challenging task of providing continuous power supply during the one-year-long MOSAiC campaign. It is therefore a recommended solution for future sea ice campaigns.

Drones proved to be a very powerful and promising tool to collect aerial measurements that are critical for an heterogenous surface such as the sea ice. Despite the many challenges met when operating close to the North Pole in freezing conditions, drones were often used when atmospheric conditions did not allow any helicopter measurements. Hence, drones enable to dramatically lower the cost and increase the temporal frequency of aerial radiation measurements compared to measurements performed via helicopters. Further development of the drone's navigation system to enable safe and automatic piloting also close to the North Pole (where the magnetic orientation is jeopardized) would be greatly beneficial.

## 3.3. NIVA

FerryBox ship of opportunity platforms are one of many types of observing platforms used in INTAROS and available for a future sustained observing system. Because ships operate along fixed transects over regular periods of time, these observations provide a high degree of spatial and temporal coverage of ocean and atmospheric observations. They are also relatively low cost since cooperation and installation of equipment is on a voluntary basis with ships that are already in operation. The core sensor package for the FerryBox system (salinity, temperature, oxygen, turbidity, and chlorophyll a fluorescence) are based on standard oceanographic sensor technology and therefore technical performance, reliability, maintenance, and data quality control and assurance (as documented by the CMEMS In-situ TAC). The advanced sensors, including the sensors for pH, $CO_3$ ion, and integrated sphere absorption are at a lower technical readiness level, but these sensors will provide a future observing system with essential ocean variables that are critical for understanding future change in the Arctic – those related to ocean acidification and functional group structure of the phytoplankton community. FerryBox platforms are one of the few observing platforms that can safely house and operate (no power/space limitations, flooding concerns, etc.) these types of sensors that can measure EOVs and emerging EOVs with measurement uncertainties that are relevant for climate change and the Arctic. The FerryBox system itself – pump, electronics, pipes, etc. – is also relatively reliable and easily maintained, and there is a European-wide implementation of >25 FerryBox systems that range from the Mediterranean Sea to the Arctic. The FerryBox and sensors for measuring core variables and advanced sensors should be included in any future sustained observing system due to the unique and low-cost generation of data from surface oceans in the Arctic. There are logistical needs related to travel to sometimes remote locations to service/maintain the ships (e.g., Longyearbyen) as well as to transmit data from shipboard computers to on shore data servers, although this is manageable using mobile internet data transfer (i.e., 3G/4G protocols). Further networking and planning is needed to identify and collaborate with ship operators in the region to increase observing efforts in the future.

## 3.4. CNRS-LOCEAN

Since more than a decade, Ocean Observing Systems have been exploiting glider capabilities to improve the observing performance in the ocean. As such, the glider contribution to INTAROS was developed in line with the international framework of the OceanGliders GOOS associated Programme which has been created to better coordinate the glider contribution in the GOOS. In particular, our glider observations fall within the objectives of specific initiatives of this programme like the Boundary Ocean Observing Network (BOON) and the Water Transformation Task Team.

Despite the remoteness and harsh environment of the Fram Strait, the INTAROS glider operations benefited from successful logistics and implementation at sea (deployment, piloting, recovery). The success is largely to be attributed to efficient collaboration within the project (for deployments and recoveries) and the high level of expertise developed in the European glider community (EGO network and EuroGOOS Glider Task Team) which enables efficient and safe glider preparation, piloting, and data management. This cooperative framework is a key element for the success of future glider-based observing systems.

As state-of-the-art gliders, the gliders implemented in INTAROS did not have navigational capabilities allowing them to cope with sea ice conditions on an operational basis. They were therefore implemented during the limited period of minimum sea ice cover during which data transmission and mission re-programming were always possible. If under ice glider navigation is feasible for short periods and distances, continuous operation of a glider in ice covered condition, which is necessary to extend the monitoring period into the fall and winter, or toward the west of the strait where major Atlantic Water recirculation and eddies are found, would require a specific permanent acoustic infrastructure to be in place. This infrastructure is needed for navigational needs (positioning) and data transmission. Data can be exchanged directly with the glider, but the glider may also be used as a “messenger” or for “data mulling' to collect data from other devices (e.g.  deep sea mooring with no surface expression). Even if the feasibility of such an infrastructure and glider performances have been demonstrated in the Fram Strait (e.g., during FP6 DAMOCLES and FP7 ACOBAR projects), installing, maintaining and operating such a system within an OOS is still a major challenge for Europe.

Glider observations in INTAROS mainly focused on the ocean physical properties. In order to extend the monitoring to biological observations miniaturized sensors suitable for gliders are needed. Such sensors have been recently developed in e.g., H2020 BRIDGES and on-going BIOGLIDERS projects, with very recent preliminary gliders cruises in the Polar Front showing the high potential of gliders for biological observations.

While several institutions in Europe (e.g., France, Norway, Poland and UK) are now reinforcing their capabilities to overcome the current limitations in glider monitoring capabilities, long term support to a better coordinated effort is still needed to consider a permanent glider component in a future Arctic Ocean Observing System.

## 3.5. CNRS-Takuvik

The use of autonomous platforms like BGC Argo floats in Arctic is a real challenge. Nevertheless, this equipment provides an interesting alternative to the collection of datasets when no sampling can be performed by a research vessel, and remote-sensing observations of the water column cannot be achieved due to ice cover.

The PRO-Ice floats turned out to be rugged and adapted to this work. The recent upgrade, with a more flexible acquisition board for the payload, promises a higher capacity of work with a larger choice of environmental sensors.

Starting in summer 2016, unprecedented datasets have been collected in Baffin Bay with a focus on seasonal changes of key biological, chemical, and physical ocean parameters. The data considerably helped to develop and improve models of the phytoplankton phenology in the Arctic and to understand the year-round evolution of the surface ocean.

So far, the BGC-Argo data collected in Baffin Bay have been exploited mostly as annual time series due to the lack of geo-localization of under-ice profiles. Interannual monitoring of the ocean state may prove difficult because of sparse float coverage (approx. 2-5 active floats each season in the entire Baffin Bay).

Under-ice positioning thus remains an issue that needs to be resolved if these data are to be used e.g., for ocean (GCM) model validation or other tasks where spatial resolution is required. Important work to estimate the float position is already in progress, but we recommend creating a dedicated working group on under-ice positioning.

## 3.6. NERSC - contributions from CAATEX to the development of an integrated Arctic Ocean Observing System

Contributors: Hanne Sagen and the CAATEX consortium.

The CAATEX project have demonstrated that the technology for a multipurpose acoustic network for basin wide thermometry, underwater geo-positioning system, and passive acoustics are at TRL-7. Furthermore, the CAATEX consortium (NERSC, WHOI, SIO) in collaboration with the crew onboard *KV Svalbard* have developed good practices for deep water mooring design for deployment and recovery in ice covered regions and procedures for recovery and deployment in deep water areas with drifting and dense sea ice.

The **mooring recovery procedure** for deep water acoustic moorings takes 1.5 – 2 days depending on the ice conditions and the visibility. The procedure developed in CAATEX has the following steps 1) Set out a couple of AIS beacons to monitor the drift, 2) Positioning of the anchor and transponders, 3) Position the pinger on the top of the mooring to learn how the mooring stands in the water column, 4) Start doing ice management  crush ice in a large area up stream relative to the anchor position , 5) Repeat the positioning of the pinger on the top to check if the mooring is moving 6) Continue ice management  crush the ice floes around the anchor position, 7) When the crushed ice field drift over the mooring position - flush and release (critical communication and timing), 8) Detect the top of the mooring and start recovering the mooring. 9) After recovery: handle the instruments and spool off wire.

The recovery procedure is developed for the deep-water moorings in CAATEX, but most of the points were also used for other moorings recovered for other parties. However, there is some key elements for safe mooring recovery that must be in place. All moorings should be equipped with a pinger on the top of the mooring as well as with locator with IRIDIUM communication, and an avalanche beacon if the mooring ends up under the ice. Furthermore, all mooring should be designed to hang as vertical as possible in the water column so that the ship can move safely towards the mooring. Based on our experience in the Beaufort Sea recoveries is that the top of the mooring should be equipped with a light which would help if a ROV can be used to locate and check the position of the mooring after release. This will make the recoveries much less risky. The successful implementation of the basin wide prototype shows that we have the technical, logistical, and operational capacity to establish a full scale multipurpose acoustic network for the central Arctic. This work and experiences will be reported as part of the CAATEX project. The future full scale acoustic network will be included in the INTAROS roadmap and will foster innovation activities within arctic observing technologies, e.g., expand the ARGO and glider programs into the ice-covered regions of the Arctic.

# 4. Summary

The deliverable D.3.13 provides an overview of distributed ocean and sea ice measurements, collected under Task 3.4 during INTAROS in different regions of the Arctic Ocean, including the central Arctic Ocean, the Barents Sea Opening, Fram Strait, deep Nansen Basin, and the Baffin Bay. Collected data sets encompass key ocean physical (temperature, salinity, and ocean currents) and biogeochemical (dissolved oxygen, pH, $pCO_2$, $CO_3$, microplastic size fractions and concentrations, Chl-a and CDOM fluorescence, nitrates, particle backscattering, absorption spectra) variables as well as sea ice properties (mass balance, thickness, ice drift) and air-snow-sea ice-ocean interfaces. The processing of *in situ* data is completed or going on and the processed and quality-controlled data products are or will be registered in the INTAROS data catalog and submitted to relevant open data bases (for some of the Task 3.4 data sets the protection period is foreseen before the releasing the full data record). Data from Task 3.4 will be delivered to data management system (and future iAOS) in WP5 and exploited in WP6 for the demonstration actions.

Table 4.1 summarizes the main objectives, field deployments, challenges, and obtained results for all in situ observing activities and technical developments by the Task 3.4 partners.

*Table 4.1. Final results obtained in Task 3.4.*

| | |
|---|---|
| **Partner** | IOPAN (in collaboration with Equipex-IAOOS) |
| **Action** | Deployment of ice-tethered IAOOS platform in the central Arctic Ocean |
| **Objective** | To provide ocean, sea ice, and atmospheric measurements in the central Arctic collected from drifting ice floe |
| **Field deployment** | Autumn 2019 in the central Arctic Ocean (close to the North Pole) |
| **Challenges** | Short-living platform, destroyed by a polar bear, problems with robustness |
| **Final results** | Monthly time series of ocean physical measurements in the upper 600 m (temperature, salinity, dissolved oxygen), temperature profiles through air-snow-sea ice-ocean (derived snow depth and ice thickness) and atmospheric measurements (air temperature and pressure, lidar observations) along the ice drift trajectory |

| | |
|---|---|
| **Partner** | IOPAN (in collaboration with UiB-GFI and NERSC) |
| **Action** | Deployment of deep ocean multidisciplinary mooring in the Nansen Basin |
| **Objective** | To provide year-round physical, biogeochemical, and acoustic measurements at fixed location from the deep basin in the Arctic Ocean |
| **Field deployment** | September 2019 to July 2020 in the deep Nansen Basin |
| **Challenges** | Difficult logistics for mooring operations in the remote, ice-cover region, recovery from under the ice, high risk mooring, no surface access. Limitation and restrictions due to COVID-19 in ship access and logistics. |
| **Final results** | Year-round measurements of physical (ocean subsurface temperature and salinity at fixed depths and profiles of ocean currents, sea ice draft and drift) and biogeochemical (dissolved oxygen, pCO2/pH) variables, passive acoustic measurements (by collaborating partners) in the Nansen Basin. Concurrent measurements with physical ocean variables collected at three CAATEX acoustic moorings |

| | |
|---|---|
| **Partner** | FMI |
| **Action** | SIMBA snow and ice mass balance buoys |
| **Objective** | To provide measurements of temperature profile through air-snow-sea ice-ocean and identify their interfaces, to collect additional data as ice floe drift trajectory, air temperature and pressure, |
| **Field deployment** | Deployment of up to 38 SIMBA buoys (partially contributed by INTAROS) during five main cruises and filed campaigns in the Arctic Ocean in 2018-2020 |
| **Challenges** | Liability and robustness of the of measurement during melting season, vulnerability of thermistor chain to ice raft and deformation, polar bear risk, unified data processing not yet available |
| **Final results** | Time series of temperature profiles in air-snow-sea ice-ocean and drift trajectories from SIMBA buoys with average lifetime of about one year, drifting mainly in the Beaufort Gyre and the Transpolar Drift Stream. Derived snow depth and ice thickness, and interface locations between snow, sea ice, and ocean |

| | |
|---|---|
| **Partner** | FMI |
| **Action** | Fixed station and UAV-based radiation measurements during the MOSAiC expedition |
| **Objective** | To collect surface broadband and spectral albedo measurements in the Central Arctic during the MOSAiC campaign |
| **Field deployment** | Fixed broadband radiation station deployed from November 2019 to November 2020. UAV-based measurements of spectral and broadband radiation (17 flights, |

| | |
|---|---|
| | corresponding to ~5 flight hours) and photography mapping of target area (35 flights, corresponding to ~11.5 flight hours) during MOSAiC leg 5 (August-October 2020). |
| **Challenges** | Cleaning pyranometers from condensation or brine/ice formation required on daily basis. Operating drones in Arctic environment (ice formation on propellers, unreliable navigation system in proximity of the North Pole, low, visibility, harsh working conditions for drone operator). Mobile target for drone measurements. |
| **Final results** | Time series and snapshots of broadband longwave and shortwave fluxes, broadband and spectral albedo, surface maps obtained from drone-based photo-mosaics |

| | |
|---|---|
| **Partner** | NIVA |
| **Action** | Novel sensors and samplers for the Barents Sea Opening FerryBox |
| **Objective** | To development and implement three different types of sampler/sensors, including a microplastics sampler, a combined deployment of spectrophotometric sensors for measuring pH and $CO_3$ ion, and an integrated sphere absorption meter sensor for measuring optical properties of seawater including dissolved organic matter and phytoplankton chlorophyll a and taxon-specific pigments for FerryBox measurements |
| **Field deployment** | Microplastic sampler deployed in 2019. Combined spectrophotometric pH/$CO_3$ system field-tested in 2018, refined in 2019 and 2020 and deployed from May 2020 to August 2021 (but offline from December 2020 to April 2021 for upgrade). Integrated sphere absorption meter sensor tested in 2019 and 2020 and installed in 2021. |
| **Challenges** | Delays in development, fabrication, installation, maintenance, and calibration due to COVID-19 (limited lab access, limited to FerryBox system, boarding restriction, limited personnel, delayed delivery of equipment). Technical issues with sensor for measuring $CO_3$ ion concentration (signal instability and high signal-to-noise ratio) and integrated sphere absorption meter sensor (LED failure). Problems with pump and flow. |
| **Final results** | Microplastic samples from several transects between Norway and Svalbard processed and analyzed. Advances made in autonomous collection of microplastics particles from seawater, assessment of ocean acidification by measuring two carbonate system variables with low volumes of seawater, and measurements of optical properties including chlorophyll, cDOM, and phytoplankton accessory pigments. FerryBox data along transects including temperature, salinity, chlorophyll a fluorescence, microplastics concentration by size fraction; seawater pH (total scale) and $CO_3$ ion concentration (µmol $kg^{-1}$) and absorption spectra ($m^{-1}$) from 360-750 nm. |

| | |
|---|---|
| **Partner** | CNRS-LOCEAN |
| **Action** | Endurance glider lines in the northern Fram Strait |
| **Objective** | To collect high resolution measurements of physical and optical ocean properties with autonomous underwater gliders along the repeated endurance lines |
| **Field deployment** | Several missions in summer/autumn seasons of 2017-2020 |
| **Challenges** | Navigation in ice-infested waters, control of glider trajectory in a strong boundary current, glider missions' time constraints (low battery autonomy, availability of recovery options) |
| **Final results** | High resolution measurements of physical (temperature and salinity) and biogeochemical (dissolved oxygen, Chl-A and CDOM fluorescence, particulate backscattering) variables in the upper 1000 m ocean column. Derived geostrophic and total depth-averaged ocean currents. |

| | |
|---|---|
| **Partner** | CNRS-Takuvik |
| **Action** | Deployments of BGC Argo floats in the Baffin Bay |
| **Objective** | To monitor biogeochemical properties of the Baffin Bay with the deployment of a fleet of BGC Argo floats dedicated to navigating in ice-infested waters |
| **Field deployment** | 17 BGC Argo deployed in 2016-2019 (deployment in 2020 cancelled) and 5 floats recovered. 4 refurbished floats to be deployed in October 2021. |
| **Challenges** | Surfacing for geo-localization and using satellite networks for data transmission and command reception in ice-covered waters. High risk, ice-detection system (ice sensing algorithm) required to make floats operational in the Arctic Ocean. Challenges related to bathymetry, ice coverage and circulation in Baffin Bay. Missing flexibility in sensor integration. |
| **Final results** | Almost 2000 profiles acquired so far with time series of physical (temperature salinity, pressure) and biogeochemical (dissolved oxygen, Chl-a and CDOM fluorescence, backscattering, nitrates) data, including under ice profiles during wintertime. Integration of new sensors (a highly sensitive radiometer and UVP6 sensor) on BGC Argo floats. |

# 5. References


Albedyll, et al, 2021. Observed seasonal evolution of the sea ice thickness distribution in the Transpolar Drift. Manuscript under final preparation. To be submitted to TC.

Athanase, M., Sennéchael, N., Garric, G., Koenig, Z., Boles, E., & Provost, C. (2019). New hydrographic measurements of the upper Arctic western Eurasian Basin in 2017 reveal fresher mixed layer and shallower warm layer than 2005–2012 climatology. Journal of Geophysical Research: Oceans, 124, 1091–1114. https://doi.org/10.1029/2018JC014701

Cheng, B., Cheng, Y., Vihma, T., Kontu, A., Zheng, F., Lemmetyinen. J., Qiu, Y. and Pulliainen, J. 2021. Inter-annual variation in lake ice composition in the European Arctic: observations based on high-resolution thermistor strings Earth Syst. Sci. Data, 13, 1–12, 2021 https://doi.org/10.5194/essd-13-1-2021.

Cheng, B., Vihma T., Rontu, L., Kontu, A. Kheyrollah Pour H., Duguay C. and Pulliainen, J. 2014. Evolution of snow and ice temperature, thickness and energy balance in Lake Orajärvi, northern Finland, Tellus A 2014, 66, 21564, http://dx.doi.org/10.3402/tellusa.v66.21564.

Cheng, Y., Cheng, B., Zheng, F., Vihma, T., Kontu, A., Yang, Q. and Liao, Z. 2020. Air/snow, snow/ice and ice/water interfaces detection from high-resolution vertical temperature profiles measured by ice mass-balance buoys on an Arctic lake. Annals of Glaciology 1–11. https://doi.org/10.1017/aog.2020.51

Hoppmann, M., M. Nicolaus, P. A. Hunkeler, P. Heil, L. K. Behrens, G. König-Langlo, and R. Gerdes. 2015. Seasonal Evolution of an Ice-Shelf Influenced Fast-Ice Regime, Derived From an Autonomous Thermistor Chain. Journal of Geophysical Research: Oceans 120: 1703–1724.

Koenig, Z., Provost, C., Villacieros- Robineau, N., Sennechael, N., & Meyer, A. (2016). Winter ocean-ice interactions under thin sea ice observed by IAOOS platforms during N-ICE2015: Salty surface mixed layer and active basal melt. Journal of Geophysical Research: Oceans, 121, 7898–7916. https://doi.org/10.1002/2016JC012195.

Koo, et al., 2021. Estimation of Thermodynamic and Dynamic Contributions to Sea Ice Growth in the Central Arctic Using ICESat-2 and MOSAiC SIMBA Buoy Data (submitted to Remote Sensing of Environment).

Krumpen, T and other 37 authors. 2020 The MOSAiC ice floe: sediment-laden survivor from the Siberian shelf, The Cryosphere, 14, 2173–2187, https://doi.org/10.5194/tc-14-2173-2020.

Le Traon P-Y, D'Ortenzio F, Babin M, Leymarie E, Marec C, Pouliquen S, Thierry V, Cabanes C, Claustre H, Desbruyères D, Lacour L, Lagunas J-L, Maze G, Mercier H, Penkerc'h C, Poffa N, Poteau A, Prieur L, Racapé V, Randelhoff A, Rehm E, Schmechtig CM, Taillandier V, Wagener T and Xing X, 2020. Preparing the New Phase of Argo: Scientific Achievements of the NAOS Project. Front. Mar. Sci. 7:577408. doi: 10.3389/fmars.2020.577408.

Lei, R., B. Cheng, P. Heil, T. Vihma, J. Wang, Q. Jiand, and Z. Zhang. 2018. Seasonal and Interannual Variations of Sea Ice Mass Balance From the Central Arctic to the Greenland Sea. Journal of Geophysical Research Oceans 123: 2422– 2439. doi:10.1002/2017JC013548.

Lei, R., Hoppmann, M., Cheng, B., Zuo, G., Gui, D., Cai, Q., Belter, H. J., and Yang, W. 2021 Seasonal changes in sea ice kinematics and deformation in the Pacific Sector of the Arctic Ocean in 2018/19, The Cryosphere, 15, 1321–1341, https://doi.org/10.5194/tc-15-1321-2021

Lei, et al, 2021 Seasonality of thermodynamic mass balance and heat fluxes of sea ice in the central Arctic during MOSAiC in 2019/20. To be submitted to Elementa.

Liao, Z., Cheng, B., Zhao, J., Vihma, T., Jackson, K., Yang, Q., Yang, Y., Zhang, L., Li, Z. Qiu, Y. and Cheng, X. 2019. Snow depth and ice thickness derived from SIMBA ice mass balance buoy data using an automated algorithm. International Journal of Digital Earth, 12:8, 962-979, DOI: 10.1080/17538947.2018.1545877.

Lusher, A., Tirelli, V., O'Connor, I. et al., 2015. Microplastics in Arctic polar waters: the first reported values of particles in surface and sub-surface samples. *Sci Rep* **5,** 14947. https://doi.org/10.1038/srep14947.

Mariage, V., Pelon, J., Blouzon, F., Victori, S., Geyskens, N., Amarouche, N., et al. (2017). Iaoos microlidar-on-buoy development and first atmospheric observations obtained during 2014 and 2015 Arctic drifts. Optics Express, 25(4), A73–A84. https://doi.org/10.1364/OE.25.000A73

Merkouriadi, I., Cheng, B., Graham, R. M., Rösel, A., & Granskog, M. A. (2017). Critical role of snow on sea ice growth in the Atlantic sector of the Arctic Ocean. Geophysical Research Letters, 44. https://doi.org/10.1002/2017GL075494.

Nicolaus, M., 2021. Overview of the MOSAiC expedition – Snow and Sea Ice. Submitted to Elementa: Science of the Anthropocene.

Provost C., N. Sennechael, J. Miguet, P. Itkin, A. Röosel, Z. Koenig, N. Villacieros-Robineau, and M. A. Granskog. 2017. Observations of Flooding and Snow-Ice Formation in a Thinner Arctic Sea-Ice Regime During the NICE2015 Campaign: Influence of Basal Ice Melt and Storms. Journal of Geophysical Research: Oceans 122: 7115–7134. doi:10.1002/2016JC012011.

Sharp, J.D. and R. Byrne, 2019. Carbonate ion concentrations in seawater: Spectrophotometric determination at ambient temperatures and evaluation of propagated calculation uncertainties. *Marine Chemistry* 209: 70-80.

--- END OF DOCUMENT ---

INTAROS

This report is made under the project
**Integrated Arctic Observation System (INTAROS)**
funded by the European Commission Horizon 2020 program
Grant Agreement no. 727890.

Project partners: